(12) INTERNATIONAL APPLICATION PUBLISHED UNDER THE PATENT COOPERATION TREATY (PCT)

(19) World Intellectual Property Organization
International Bureau

(43) International Publication Date
14 September 2017 (14.09.2017)

WIPO | PCT

(10) International Publication Number
WO 2017/156362 A1

(51) International Patent Classification:
C12N 15/113 (2010.01) *C12Q 1/68* (2006.01)
A61P 37/02 (2006.01) *G01N 33/573* (2006.01)

(21) International Application Number:
PCT/US2017/021727

(22) International Filing Date:
10 March 2017 (10.03.2017)

(25) Filing Language: English

(26) Publication Language: English

(30) Priority Data:
62/307,124 11 March 2016 (11.03.2016) US

(71) Applicant: **PRESIDENT AND FELLOWS OF HARVARD COLLEGE** [US/US]; 17 Quincy Street, Cambridge, MA 02138 (US).

(72) Inventors: **RON-HAREL, Noga**; 50 Green Street, Apt. 302, Brookline, MA 02446 (US). **HAIGIS, Marcia C.**; 16 Madison Avenue, Winchester, MA 01890 (US).

(74) Agents: **SMITH, DeAnn F.** et al.; Patent Group, Foley Hoag LLP, 155 Seaport Blvd., Boston, MA 02210-2600 (US).

(81) Designated States *(unless otherwise indicated, for every kind of national protection available)*: AE, AG, AL, AM, AO, AT, AU, AZ, BA, BB, BG, BH, BN, BR, BW, BY, BZ, CA, CH, CL, CN, CO, CR, CU, CZ, DE, DJ, DK, DM, DO, DZ, EC, EE, EG, ES, FI, GB, GD, GE, GH, GM, GT, HN, HR, HU, ID, IL, IN, IR, IS, JP, KE, KG, KH, KN, KP, KR, KW, KZ, LA, LC, LK, LR, LS, LU, LY, MA, MD, ME, MG, MK, MN, MW, MX, MY, MZ, NA, NG, NI, NO, NZ, OM, PA, PE, PG, PH, PL, PT, QA, RO, RS, RU, RW, SA, SC, SD, SE, SG, SK, SL, SM, ST, SV, SY, TH, TJ, TM, TN, TR, TT, TZ, UA, UG, US, UZ, VC, VN, ZA, ZM, ZW.

(84) Designated States *(unless otherwise indicated, for every kind of regional protection available)*: ARIPO (BW, GH, GM, KE, LR, LS, MW, MZ, NA, RW, SD, SL, ST, SZ, TZ, UG, ZM, ZW), Eurasian (AM, AZ, BY, KG, KZ, RU, TJ, TM), European (AL, AT, BE, BG, CH, CY, CZ, DE, DK, EE, ES, FI, FR, GB, GR, HR, HU, IE, IS, IT, LT, LU, LV, MC, MK, MT, NL, NO, PL, PT, RO, RS, SE, SI, SK, SM, TR), OAPI (BF, BJ, CF, CG, CI, CM, GA, GN, GQ, GW, KM, ML, MR, NE, SN, TD, TG).

Published:

— *with international search report (Art. 21(3))*

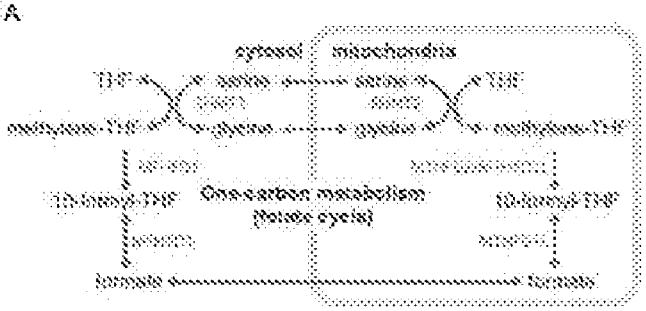
— *before the expiration of the time limit for amending the claims and to be republished in the event of receipt of amendments (Rule 48.2(h))*

WO 2017/156362 A1

(54) Title: MODULATING T CELL SURVIVAL BY TARGETING THE ONE-CARBON METABOLIC PATHWAY

Figure 10

A



(57) Abstract: Provided herein are therapeutic and diagnostic methods related to the targeting of the one-carbon metabolic pathway in T cells.

MODULATING T CELL SURVIVAL BY TARGETING THE ONE-CARBON METABOLIC PATHWAY

RELATED APPLICATIONS

This application claims the benefit of priority to U.S. Provisional Application No. 62/307,124, filed March 11, 2016, which is hereby incorporated in its entirety.

BACKGROUND

To support proliferation, activated T cells, like tumor cells, utilize metabolic reprogramming to generate precursors required for macromolecular synthesis, energy, stress response and other pro-survival pathways. In proliferating cells, glucose provides a major fuel source and is diverted away from simple mitochondrial oxidative metabolism into pathways that contribute to anabolic synthesis and NADPH production. To initiate an immune response against pathogens, a small number of antigen-specific T cells within the polyclonal repertoire need to proliferate rapidly to generate large amounts of effector cells that can clear pathogens. In T cells, exit from quiescence and entry into the cell cycle is determined by external cues of activation, which also regulate the switch from catabolic to anabolic metabolism. For instance, upon naïve T cell activation, signaling pathways downstream of the T cell receptor through Erk and downstream of the CD28 costimulatory receptor through phosphatidylinositol 3'-kinase (PI3K)/Akt, stimulate glucose and glutamine uptake and metabolism.

Mitochondria are not inert during metabolic rewiring and play an active role in anabolic metabolism through export of glucose-derived citrate for lipid biosynthesis, as well as in signaling, in part, through reactive oxygen species (ROS)-stimulated cytokine production. However, the full extent of mitochondrial reprogramming important for sustaining T cell activation and survival remains undetermined.

SUMMARY

In some aspects, provided herein are agents, compositions (e.g., compositions comprising agents described herein) and methods of treating diseases or disorders (e.g., autoimmune, immune related disorders, and/or cancer) by modulating the one-carbon metabolic pathway. In some embodiments, provided herein are methods of determining the efficacy of an immunotherapy in a subject comprising detecting the level of SHMT1,

SHMT2, MTHFD1, MTHFD2, MTHFD1L or MTHFD2L expressed by T cells in the subject. In some aspects, provided herein are methods of detecting T cell exhaustion in a subject comprising detecting the level of SHMT1, SHMT2, MTHFD1, MTHFD2, MTHFD1L or MTHFD2L expressed by T cells in the subject.

Also provided herein provided herein are methods of increasing tumor infiltrating T cell activity and/or function in a subject comprising administering to the subject an agent that increases the activity or expression of SHMT1, SHMT2, MTHFD1, MTHFD1L, MTHFD2, MTHFD2L, FPGS, TYMS, DHFR, MTHFS, or MTRR in the subject. Additionally, provided herein are methods of reducing age-related T cell dysfunction or increasing T cell growth in a subject by administering to the subject an agent that activates to the one-carbon pathway.

Definitions

For convenience, certain terms employed in the specification, examples, and appended claims are collected here.

As used herein, the term "*administering*" means providing an agent or composition to a subject, and includes, but is not limited to, administering by a medical professional and self-administering.

The term "*agent*" is used herein to denote a chemical compound, a small molecule, a mixture of chemical compounds and/or a biological macromolecule (such as a nucleic acid, a protein, or a peptide). The activity of such agents may render them suitable as a "therapeutic agent" which is a biologically, physiologically, or pharmacologically active substance (or substances) that acts locally or systemically in a subject.

The terms "*polynucleotide*", and "*nucleic acid*" are used interchangeably. They refer to a polymeric form of nucleotides of any length, either deoxyribonucleotides or ribonucleotides, or analogs thereof. Polynucleotides may have any three-dimensional structure, and may perform any function, known or unknown. The following are non-limiting examples of polynucleotides: coding or non-coding regions of a gene or gene fragment, loci (locus) defined from linkage analysis, exons, introns, messenger RNA (mRNA), transfer RNA, ribosomal RNA, ribozymes, cDNA, recombinant polynucleotides, branched polynucleotides, plasmids, vectors, isolated DNA of any sequence, isolated RNA of any sequence, nucleic acid probes, and primers. A polynucleotide may comprise modified nucleotides, such as methylated nucleotides and nucleotide analogs. If present, modifications to the nucleotide structure may be imparted before or after assembly of the

polymer. The sequence of nucleotides may be interrupted by non-nucleotide components. A polynucleotide may be further modified, such as by conjugation with a labeling component. The term "recombinant" polynucleotide means a polynucleotide of genomic, cDNA, semisynthetic, or synthetic origin which either does not occur in nature or is linked to another polynucleotide in a non-natural arrangement.

The phrase "*pharmaceutically-acceptable carrier*" as used herein means a pharmaceutically-acceptable material, composition or vehicle, such as a liquid or solid filler, diluent, excipient, or solvent encapsulating material, involved in carrying or transporting the subject compound from one organ, or portion of the body, to another organ, or portion of the body.

As used herein, a therapeutic that "*prevents*" a disorder or condition refers to a compound that, when administered to a statistical sample prior to the onset of the disorder or condition, reduces the occurrence of the disorder or condition in the treated sample relative to an untreated control sample, or delays the onset or reduces the severity of one or more symptoms of the disorder or condition relative to the untreated control sample.

The term "*small molecule*" is a term of the art and includes molecules that are less than about 1000 molecular weight or less than about 500 molecular weight. In one embodiment, small molecules do not exclusively comprise peptide bonds. In another embodiment, small molecules are not oligomeric. Exemplary small molecule compounds which can be screened for activity include, but are not limited to, peptides, peptidomimetics, nucleic acids, carbohydrates, small organic molecules (*e.g.*, polyketides) (Cane *et al.* (1998) *Science* 282:63), and natural product extract libraries. In another embodiment, the compounds are small, organic non-peptidic compounds. In a further embodiment, a small molecule is not biosynthetic.

As used herein, the term "*subject*" means a human or non-human animal selected for treatment or therapy.

"*Treating*" a disease in a subject or "*treating*" a subject having a disease refers to subjecting the subject to a pharmaceutical treatment, *e.g.*, the administration of a drug, such that at least one symptom of the disease is decreased or prevented from worsening.

Indications

In one aspect, provided herein is a method of treating or preventing an autoimmune disease, an inflammatory disease, a graft-versus host disease or organ transplant rejection in

a subject, wherein the method comprises administering to the subject an agent that inhibits the one-carbon metabolic pathway. In certain embodiments, the agent inhibits the activity or expression of SHMT1, SHMT2, MTHFD1, MTHFD2, MTHFD1L or MTHFD2L. In some embodiments the one-carbon metabolic pathway is inhibited in T cells in the subject. In certain embodiments, the inhibition of the one-carbon metabolic pathway in the T cells of the subject reduces T cell survival in the subject.

In some embodiments, the agent is a small molecule. In certain embodiments, the agent is an inhibitory polynucleotide (*e.g.*, siRNA, shRNA, and an antisense RNA molecule, such as an inhibitory polynucleotide that targets SHMT1 mRNA, SHMT2 mRNA, MTHFD1 mRNA, MTHFD2 mRNA, MTHFD1L mRNA or MTHFD2L mRNA). In some embodiments, the agent is a polynucleotide that encodes a molecule selected from siRNA, shRNA, and an antisense RNA molecule. Examples of agents that inhibit the one-carbon metabolic pathway disclosed in International Patent Application Publications WO 2015/160470, WO 2015/00302 and WO 2014/150688 and U.S. Patent Application Publications US2016/0032401 and US 2015/0011611, each of which are hereby incorporated by reference in their entirety.

In some embodiments, the method comprises the treatment of an autoimmune disease. In some embodiments, the autoimmune disease is selected from the group consisting of glomerular nephritis, arthritis, dilated cardiomyopathy-like disease, ulceous colitis, Sjogren syndrome, Crohn's disease, systemic erythematodes, chronic rheumatoid arthritis, multiple sclerosis, psoriasis, allergic contact dermatitis, polymyosiis, pachyderma, periarteritis nodosa, rheumatic fever, vitiligo vulgaris, insulin dependent diabetes mellitus, Behcet disease, Hashimoto disease, Addison disease, dermatomyositis, myasthenia gravis, Reiter syndrome, Graves' disease, anaemia perniciosa, Goodpasture syndrome, sterility disease, chronic active hepatitis, pemphigus, autoimmune thrombopenic purpura, and autoimmune hemolytic anemia, active chronic hepatitis, Addison's disease, anti-phospholipid syndrome, atopic allergy, autoimmune atrophic gastritis, achlorhydra autoimmune, celiac disease, Cushing's syndrome, dermatomyositis, discoid lupus, erythematosis, Hashimoto's thyroiditis, idiopathic adrenal atrophy, idiopathic thrombocytopenia, insulin-dependent diabetes, Lambert-Eaton syndrome, lupoid hepatitis, some cases of lymphopenia, mixed connective tissue disease, pemphigoid, pemphigus vulgaris, pernicious anema, phacogenic uveitis, polyarteritis nodosa, polyglandular autosyndromes, primary biliary cirrhosis, primary sclerosing cholangitis, Raynaud's syndrome, relapsing polychondritis, Schmidt's syndrome,

limited scleroderma (or crest syndrome), sympathetic ophthalmia, systemic lupus erythematosis, Takayasu's arteritis, temporal arteritis, thyrotoxicosis, type b insulin resistance, ulcerative colitis and Wegener's granulomatosis.

In some embodiments, the method comprises the treatment of an inflammatory disease. In some embodiments, the inflammatory disease is selected from the group consisting of inflammatory bowel disease, rheumatoid arthritis, psoriatic arthritis, psoriasis, diabetes mellitus, Alzheimer's disease, refractory asthma, multiple sclerosis, atherosclerosis, and vasculitis. In some embodiments, the inflammatory disease is an inflammatory bowel disease. In some embodiments, the inflammatory bowel disease is selected from the group consisting of Crohn's disease, ulcerative colitis, irritable bowel syndrome, microscopic colitis, lymphocytic-plasmocytic enteritis, coeliac disease, collagenous colitis, lymphocytic colitis and eosinophilic enterocolitis.

In certain aspects, provided herein is a method of treating or preventing a disease or disorder associated with impairment of the one-carbon metabolic pathway in a subject comprising administering to the subject an agent that increases the activity or expression of SHMT1, SHMT2, MTHFD1, MTHFD2, MTHFD1L or MTHFD2L in the subject. In certain embodiments, the agent increases the activity or expression of SHMT1, SHMT2, MTHFD1, MTHFD2, MTHFD1L or MTHFD2L in T cells of the subject. In certain embodiments, the agent is a small molecule. In some embodiments, the small molecule increases the activity of SHMT1, SHMT2, MTHFD1, MTHFD2, MTHFD1L or MTHFD2L. In certain embodiments, the agent is a polynucleotide. In some embodiments, the polynucleotide encodes SHMT1, SHMT2, MTHFD1, MTHFD2, MTHFD1L or MTHFD2L. In some embodiments, the polynucleotide is in a vector. In some embodiments, the vector is a viral vector, a retroviral vector, a bacterial vector or a plasmid vector. In some embodiments, the polynucleotide is an mRNA.

In certain embodiments, the subject has an impaired immune system. In some embodiments, the subject has reduced numbers of activated T cells. In some embodiments, the subject has a disease or disorder selected from the group consisting of Smith-Magenis Syndrome (SHMT1 deletion), MTHFR deficiency, MTHFD1 deficiency, schizophrenia (MTHFR polymorphism), depression (methionine sulfoxide reductase), AD-MTHFR and MTR polymorphism, cobalamine deficiency and transcobalamine deficiency.

In certain embodiments of the methods provided herein, the subject is a human subject. In some embodiments, the agent is administered to the subject intravenously, intramuscularly, intraperitoneally, subcutaneously or orally.

In certain aspects, provided herein is a method of detecting T cell activation comprising detecting the level of SHMT1, SHMT2, MTHFD1, MTHFD2, MTHFD1L or MTHFD2L in a T cell.

In certain aspects, provided herein is a method of detecting an autoimmune disease, an inflammatory disease, a graft-versus host disease or organ transplant rejection in a subject comprising detecting the level of SHMT1, SHMT2, MTHFD1, MTHFD2, MTHFD1L or MTHFD2L expressed by T cells in the subject.

In certain aspects, provided herein is a method of determining the efficacy of an immunotherapy in a subject comprising detecting the level of SHMT1, SHMT2, MTHFD1, MTHFD2, MTHFD1L or MTHFD2L expressed by T cells in the subject. In some embodiments, the subject has cancer.

In some aspects, provided herein is a method of detecting T cell exhaustion in a subject comprising detecting the level of SHMT1, SHMT2, MTHFD1, MTHFD2, MTHFD1L or MTHFD2L expressed by T cells in the subject. In some embodiments, the level of T cell exhaustion is being detected to determine whether the subject is a suitable candidate for an immunotherapy.

In certain embodiments of the methods provided herein, the level of SHMT1, SHMT2, MTHFD1, MTHFD2, MTHFD1L or MTHFD2L is detected using an antibody that specifically binds to SHMT1, SHMT2, MTHFD1, MTHFD2, MTHFD1L or MTHFD2L. In some embodiments, the antibody is detectably labeled (e.g., a fluorescent label). In certain embodiments, the level of SHMT1, SHMT2, MTHFD1, MTHFD2, MTHFD1L or MTHFD2L is detected by flow cytometry or fluorescent microscopy. In certain embodiments, the T cell is in a tissue sample. In some embodiments, the tissue sample is a tumor biopsy sample, or a lymph node biopsy sample. In certain embodiments, the T cell is from a blood sample.

In certain embodiments, the immunotherapy comprises administering an immune checkpoint inhibitor to the subject. In some embodiments, the immune checkpoint inhibitor is an antibody or antigen-binding fragment thereof that specifically binds to an immune checkpoint protein. In some embodiments, the immune checkpoint protein is selected from the group consisting of CTLA4, PD-1, PD-L1, PD-L2, A2AR, B7-H3, B7-H4, BTLA, KIR,

LAG3, TIM-3 or VISTA. In some embodiments, the immune checkpoint inhibitor is selected from the group consisting of nivolumab, pembrolizumab, pidilizumab, AMP-224, AMP-514, STI-A1110, TSR-042, RG-7446, BMS-936559, MEDI-4736, MSB-0020718C, AUR-012 and STI-A1010. In certain embodiments, immunotherapy is a vaccine. In certain embodiments, the immunotherapy comprises administering a cancer vaccine to the subject. In some embodiments, the immunotherapy comprises administering a cancer-specific T cell to the subject. In some embodiments, the cancer-specific T cell expresses a chimeric antigen receptor. In certain embodiments, the immunotherapy comprises administering an adjuvant to the subject. In some embodiments, the adjuvant is selected from the group consisting of an immune modulatory protein, Adjuvant 65, α-GalCer, aluminum phosphate, aluminum hydroxide, calcium phosphate, β-Glucan Peptide, CpG DNA, GPI-0100, lipid A, lipopolysaccharide, Lipovant, Montanide, N-acetyl-muramyl-L-alanyl-D-isoglutamine, Pam3CSK4, quil A and trehalose dimycolate.

In certain embodiments of the methods provided herein, the subject is a human subject. In some embodiments, the subject has cancer. In some embodiments, the subject is elderly.

In some aspects, provide herein are methods of treating or preventing a cancer (e.g., a cancer associated with impaired or dysfunctional one-carbon metabolism) in a subject comprising administering to the subject an agent or a composition (e.g., a composition comprising an agent) that increases the activity or expression of SHMT1, SHMT2, MTHFD1, MTHFD1L, MTHFD2, MTHFD2L, FPGS, TYMS, DHFR, MTHFS, or MTRR in the subject. In certain embodiments, the agent increases the activity or expression of SHMT1, SHMT2, MTHFD1, MTHFD1L, MTHFD2, MTHFD2L, FPGS, TYMS, DHFR, MTHFS, or MTRR in T cells of the subject.

In certain embodiments, the agent is a small molecule. In some embodiments, the small molecule increases the activity of SHMT1, SHMT2, MTHFD1, MTHFD1L, MTHFD2, MTHFD2L, FPGS, TYMS, DHFR, MTHFS, or MTRR. In certain embodiments, the agent is a polynucleotide. In some embodiments, the polynucleotide encodes SHMT1, SHMT2, MTHFD1, MTHFD1L, MTHFD2, MTHFD2L, FPGS, TYMS, DHFR, MTHFS, or MTRR. In some embodiments, the polynucleotide is in a vector. In some embodiments, the vector is a viral vector, a retroviral vector, a bacterial vector or a plasmid vector. In some embodiments, the polynucleotide is an mRNA.

Tumor infiltrating Tregs (TITRs) are known to infiltrate cancerous tumors and are believed to play a role in the suppression of a host's immune response against infiltrated tumors. Therefore, TITRs are an attractive therapeutic target for the treatment of cancer. In some aspects, provided herein are methods of increasing tumor infiltrating T cell activity and/or function in a subject comprising administering to the subject an agent that increases the activity or expression of SHMT1, SHMT2, MTHFD1, MTHFD1L, MTHFD2, MTHFD2L, FPGS, TYMS, DHFR, MTHFS, or MTRR in the subject. Also provided herein are methods of treating a tumor in a subject by administering to the subject an agent that increases the activity or expression of SHMT1, SHMT2, MTHFD1, MTHFD1L, MTHFD2, MTHFD2L, FPGS, TYMS, DHFR, MTHFS, or MTRR in the subject.

In some aspects, provided herein are methods of treating a cancer by administering to a subject (e.g., to a tumor present in a subject) an agent described herein.

In some embodiments, the methods described herein may be used to treat any cancerous or pre-cancerous tumor. In some embodiments, the cancer includes a solid tumor. Cancers that may be treated by methods and compositions provided herein include, but are not limited to, cancer cells from the bladder, blood, bone, bone marrow, brain, breast, colon, esophagus, gastrointestine, gum, head, kidney, liver, lung, nasopharynx, neck, ovary, prostate, skin, stomach, testis, tongue, or uterus. In addition, the cancer may specifically be of the following histological type, though it is not limited to these: neoplasm, malignant; carcinoma; carcinoma, undifferentiated; giant and spindle cell carcinoma; small cell carcinoma; papillary carcinoma; squamous cell carcinoma; lymphoepithelial carcinoma; basal cell carcinoma; pilomatrix carcinoma; transitional cell carcinoma; papillary transitional cell carcinoma; adenocarcinoma; gastrinoma, malignant; cholangiocarcinoma; hepatocellular carcinoma; combined hepatocellular carcinoma and cholangiocarcinoma; trabecular adenocarcinoma; adenoid cystic carcinoma; adenocarcinoma in adenomatous polyp; adenocarcinoma, familial polyposis coli; solid carcinoma; carcinoid tumor, malignant; branchiolo-alveolar adenocarcinoma; papillary adenocarcinoma; chromophobe carcinoma; acidophil carcinoma; oxyphilic adenocarcinoma; basophil carcinoma; clear cell adenocarcinoma; granular cell carcinoma; follicular adenocarcinoma; papillary and follicular adenocarcinoma; nonencapsulating sclerosing carcinoma; adrenal cortical carcinoma; endometrioid carcinoma; skin appendage carcinoma; apocrine adenocarcinoma; sebaceous adenocarcinoma; ceruminous adenocarcinoma; mucoepidermoid carcinoma; cystadenocarcinoma; papillary cystadenocarcinoma; papillary serous cystadenocarcinoma;

mucinous cystadenocarcinoma; mucinous adenocarcinoma; signet ring cell carcinoma; infiltrating duct carcinoma; medullary carcinoma; lobular carcinoma; inflammatory carcinoma; mammary paget's disease; acinar cell carcinoma; adenosquamous carcinoma; adenocarcinoma w/squamous metaplasia; malignant thymoma; malignant ovarian stromal tumor; malignant thecoma; malignant granulosa cell tumor; and malignant roblastoma; sertoli cell carcinoma; malignant leydig cell tumor; malignant lipid cell tumor; malignant paraganglioma; malignant extra-mammary paraganglioma; pheochromocytoma; glomangiosarcoma; malignant melanoma; amelanotic melanoma; superficial spreading melanoma; malignant melanoma in giant pigmented nevus; epithelioid cell melanoma; malignant blue nevus; sarcoma; fibrosarcoma; malignant fibrous histiocytoma; myxosarcoma; liposarcoma; leiomyosarcoma; rhabdomyosarcoma; embryonal rhabdomyosarcoma; alveolar rhabdomyosarcoma; stromal sarcoma; malignant mixed tumor; mullerian mixed tumor; nephroblastoma; hepatoblastoma; carcinosarcoma; malignant mesenchymoma; malignant brenner tumor; malignant phyllodes tumor; synovial sarcoma; malignant mesothelioma; dysgerminoma; embryonal carcinoma; malignant teratoma; malignant struma ovarii; choriocarcinoma; malignant mesonephroma; hemangiosarcoma; malignant hemangioendothelioma; kaposi's sarcoma; malignant hemangiopericytoma; lymphangiosarcoma; osteosarcoma; juxtacortical osteosarcoma; chondrosarcoma; malignant chondroblastoma; mesenchymal chondrosarcoma; giant cell tumor of bone; ewing's sarcoma; malignant odontogenic tumor; ameloblastic odontosarcoma; malignant ameloblastoma; ameloblastic fibrosarcoma; malignant pinealoma; chordoma; malignant glioma; ependymoma; astrocytoma; protoplasmic astrocytoma; fibrillary astrocytoma; astroblastoma; glioblastoma; oligodendroglioma; oligodendroblastoma; primitive neuroectodermal; cerebellar sarcoma; ganglioneuroblastoma; neuroblastoma; retinoblastoma; olfactory neurogenic tumor; malignant meningioma; neurofibrosarcoma; malignant neurilemmoma; malignant granular cell tumor; malignant lymphoma; Hodgkin's disease; Hodgkin's lymphoma; paragranuloma; small lymphocytic malignant lymphoma; diffuse large cell malignant lymphoma; follicular malignant lymphoma; mycosis fungoides; other specified non-Hodgkin's lymphomas; malignant histiocytosis; multiple myeloma; mast cell sarcoma; immunoproliferative small intestinal disease; leukemia; lymphoid leukemia; plasma cell leukemia; erythroleukemia; lymphosarcoma cell leukemia; myeloid leukemia; basophilic leukemia; eosinophilic leukemia; monocytic leukemia; mast cell leukemia; megakaryoblastic leukemia; myeloid sarcoma; and hairy cell leukemia.

In some embodiments, the subject has cancer. In some embodiments, the cancer comprises a solid tumor. In some embodiments, the tumor is an adenocarcinoma, an adrenal tumor, an anal tumor, a bile duct tumor, a bladder tumor, a bone tumor, a blood born tumor, a brain/CNS tumor, a breast tumor, a cervical tumor, a colorectal tumor, an endometrial tumor, an esophageal tumor, an Ewing tumor, an eye tumor, a gallbladder tumor, a gastrointestinal, a kidney tumor, a laryngeal or hypopharyngreal tumor, a liver tumor, a lung tumor, a mesothelioma tumor, a multiple myeloma tumor, a muscle tumor, a nasopharyngeal tumor, a neuroblastoma, an oral tumor, an osteosarcoma, an ovarian tumor, a pancreatic tumor, a penile tumor, a pituitary tumor, a primary tumor, a prostate tumor, a retinoblastoma, a Rhabdomyosarcoma, a salivary gland tumor, a soft tissue sarcoma, a melanoma, a metastatic tumor, a basal cell carcinoma, a Merkel cell tumor, a testicular tumor, a thymus tumor, a thyroid tumor, a uterine tumor, a vaginal tumor, a vulvar tumor, or a Wilms tumor.

Age associated decline of the immune system (e.g., an increase in age-related T cell dysfunction) can be a health concern. All components of innate and adaptive immunity are adversely affected to lesser or greater extent by ageing resulting in an overall decline of immunocompetence. As a result, in the aged population, there is increased susceptibility to infection, poor responses to vaccination, and increased incidence of autoreactivity. There is an increasing focus on the role of T cells during ageing because of their impact on the overall immune responses. A steady decline in the production of T cells, more restricted T cell receptor (TCR) repertoire, a decline in T cell growth, and weak activation of T cells are some of the effects of ageing. Provided herein are methods of reducing, inhibiting, or preventing age-related T cell dysfunction in a subject by administering to the subject an agent that increases the activity or expression of SHMT1, SHMT2, MTHFD1, MTHFD1L, MTHFD2, MTHFD2L, FPGS, TYMS, DHFR, MTHFS, or MTRR in the subject. Also provided herein are methods of increasing T cell growth associated with the one-carbon metabolic pathway by administering to the subject an agent that increases the activity or expression of SHMT1, SHMT2, MTHFD1, MTHFD1L, MTHFD2, MTHFD2L, FPGS, TYMS, DHFR, MTHFS, or MTRR in the subject. In certain embodiments, the agent increases the activity or expression of SHMT1, SHMT2, MTHFD1, MTHFD1L, MTHFD2, MTHFD2L, FPGS, TYMS, DHFR, MTHFS, or MTRR in T cells of the subject. In some embodiments, the agent is a metabolite. In some embodiments, the agent is formate. The agent may be an antioxidant (e.g., a glutathione precursor such as N-acetyl-L-cysteine). In

some embodiments, two or more, three or more, four or more, or five or more agents may be used.

An agent or composition described herein may be administered by any means known in the art. For example, the agent may be administered intravenously, intramuscularly, orally, or locally. In some embodiments, the agents and/or compositions are delivered locally. The agents and/or compositions (e.g., pharmaceutical compositions) may be administered to a tumor present in the subject.

In some embodiments, the agent and/or composition is administered with an additional agent or therapy (e.g., a therapy used to treat cancer, such as a cancer vaccine). In some embodiments, the additional agent is a chemotherapeutic agent. Exemplary chemotherapeutic agents include alkylating agents such as thiotepa and cyclophosphamide (Cytoxan™); alkyl sulfonates such as busulfan, improsulfan and piposulfan; aziridines such as benzodopa, carboquone, meturedopa, and uredopa; emylerumines and memylamelamines including alfretamine, triemylenemelamine, triethylenephosphoramide, triethylenethiophosphoramide, and trimemylolomelamine; acetogenins (especially bullatacin and bullatacinone); a camptothecin (including synthetic analogue topotecan); bryostatin; callystatin; CC-1065 (including its adozelesin, carzelesin and bizelesin synthetic analogues); cryptophycins (articularly cryptophycin 1 and cryptophycin 8); dolastatin; duocarmycin (including the synthetic analogues, KW-2189 and CBI-TMI); eleutherobin; pancratistatin; a sarcodictyin; spongistatin; nitrogen mustards such as chlorambucil, chlornaphazine, cholophosphamide, estramustine, ifosfamide, mechlorethamine, mechlorethamine oxide hydrochloride, melphalan, novembichin, phenesterine, prednimustine, trofosfamide, uracil mustard; nitrosoureas such as carmustine, chlorozotocin, foremustine, lomustine, nimustine, ranimustine; antibiotics such as the enediyne antibiotics (e.g., calicheamicin, especially calicheamicin gammall and calicheamicin phili); dynemicin, including dynemicin A; bisphosphonates, such as clodronate; an esperamicin; as well as neocarzinostatin chromophore and related chromoprotein enediyne antibiotic chromomophores), aclacinomysins, actinomycin, authramycin, azaserine, bleomycins, cactinomycin, carabicin, carminomycin, carzinophilin, chromomycins, dactinomycin, daunorubicin, detorubicin, 6-diazo-5-oxo-L-norleucine, doxorubicin (Adramycin™) (including morpholino-doxorubicin, cyanomorpholino-doxorubicin, 2-pyrrolino-doxorubicin and deoxydoxorubicin), epirubicin, esorubicin, idarubicin, marcellomycin, mitomycins such as mitomycin C, mycophenolic acid, nogalamycin, olivomycins, peplomycin, potfiromycin, puromycin, quelamycin,

rodorubicin, streptonigrin, streptozocin, tubercidin, ubenimex, zinostatin, zorubicin; anti-metabolites such as methotrexate and 5-fluorouracil (5-FU); folic acid analogues such as demopterin, methotrexate, pteropterin, trimetrexate; purine analogs such as fludarabine, 6-mercaptopurine, thiamiprine, thioguanine; pyrimidine analogues such as ancitabine, azacitidine, 6-azauridine, carmofur, cytarabine, dideoxyuridine, doxifluridine, enocitabine, floxuridine; androgens such as calusterone, dromostanolone propionate, epitiostanol, mepitiostane, testolactone; anti-adrenals such as aminoglutethimide, mitotane, trilostane; folic acid replinisher such as frolinic acid; aceglatone; aldophosphamide glycoside; aminolevulinic acid; eniluracil; amsacrine; hestrabucil; bisantrene; edatraxate; defofamine; demecolcine; diaziquone; elformthine; elliptinium acetate; an epothilone; etoglucid; gallium nitrate; hydroxyurea; lentinan; lonidamine; maytansinoids such as maytansine and ansamitocins; mitoguazone; mitoxantrone; mopidamol; nitracrine; pentostatin; phenamet; pirarubicin; losoxantrone; podophyllinic acid; 2-ethylhydrazide; procarbazine; PSK™; razoxane; rhizoxin; sizofiran; spirogermanium; tenuazonic acid; triaziquone; 2,2',2''-tricUorotriemylamine; trichothecenes (especially T-2 toxin, verracurin A, roridin A and anguidine); urethane; vindesine; dacarbazine; mannomustine; mitobronitol; mitolactol; pipobroman; gacytosine; arabinoside ("Ara-C"); cyclophosphamide; thiopeta; taxoids, e.g., paclitaxel (Taxol™, Bristol Meyers Squibb Oncology, Princeton, N.J.) and docetaxel (Taxoteret™, Rhone-Poulenc Rorer, Antony, France); chlorambucil; gemcitabine (Gemzar™); 6-thioguanine; mercaptopurine; methotrexate; platinum analogs such as cisplatin and carboplatin; vinblastine; platinum; etoposide (VP-16); ifosfamide; mitroxantrone; vancristine; vinorelbine (Navelbine™); novantrone; teniposide; edatrexate; daunomycin; aminopterin; xeoloda; ibandronate; CPT-11; topoisomerase inhibitor RFS 2000; difluoromethylornithine (DMFO); retinoids such as retinoic acid; capecitabine; and pharmaceutically acceptable salts, acids or derivatives of any of the above. Also included in the definition of "chemotherapeutic agent" are anti-hormonal agents that act to regulate or inhibit hormone action on tumors such as anti-estrogens and selective estrogen receptor modulators (SERMs), including, for example, tamoxifen (including Nolvadex™), raloxifene, droloxifene, 4-hydroxytamoxifen, trioxifene, keoxifene, LY117018, onapristone, and toremifene (Fareston™); inhibitors of the enzyme aromatase, which regulates estrogen production in the adrenal glands, such as, for example, 4(5)-imidazoles, aminoglutethimide, megestrol acetate (Megace™), exemestane, formestane, fadrozole, vorozole (Rivisor™), letrozole (Femara™), and anastrozole (Arimidex™); and anti-androgens such as flutamide,

nilutamide, bicalutamide, leuprohde, and goserelin; and pharmaceutically acceptable salts, acids or derivatives of any of the above. In some embodiments, the additional therapeutic agent is an immune checkpoint inhibitor. Immune checkpoint inhibition broadly refers to inhibiting the checkpoints that cancer cells can produce to prevent or downregulate an immune response. Examples of immune checkpoint proteins are CTLA-4, PD-1, VISTA, B7-H2, B7-H3, PD-L1, B7-H4, B7-H6, ICOS, HVEM, PD-L2, CD160, gp49B, PIR-B, KIR family receptors, TIM-1, TIM-3, TIM-4, LAG-3, BTLA, SIRPalpha (CD47), CD48, 2B4 (CD244), B7.1, B7.2, ILT-2, ILT-4, TIGIT, HHLA2, butyrophilins, A2aR, and combinations thereof.

Actual dosage levels of the agents to be administered may be varied so as to obtain an amount of the active ingredient (e.g., an agent described herein) which is effective to achieve the desired therapeutic response for a particular patient, composition, and mode of administration, without being toxic to the patient.

The selected dosage level will depend upon a variety of factors including the activity of the particular agent employed, the route of administration, the time of administration, the rate of excretion or metabolism of the particular compound being employed, the duration of the treatment, other drugs, compounds and/or materials used in combination with the particular compound employed, the age, sex, weight, condition, general health and prior medical history of the patient being treated, and like factors well known in the medical arts.

A physician or veterinarian having ordinary skill in the art can readily determine and prescribe the effective amount of the agent and/or pharmaceutical composition required. For example, the physician or veterinarian could prescribe and/or administer doses of the compounds employed in the agent and/or pharmaceutical composition at levels lower than that required in order to achieve the desired therapeutic effect and gradually increase the dosage until the desired effect is achieved.

Pharmaceutical Compositions

In some aspects, provided herein are methods and compositions to treat diseases and disorders in a subject by modulating the one-carbon metabolic pathway in a subject. In some aspects, provided herein are methods and compositions to modulate T cell growth or T cell activity (e.g., reduce the T cell dysfunction) in a subject. In some embodiments, the agents are formulated with a pharmaceutically acceptable carrier. In some embodiments, the pharmaceutical composition is delivered locally or systemically. In some embodiments, the

pharmaceutical composition may be administered to a tumor present in the subject. In some embodiments, the agent or pharmaceutical composition is administered with a second cancer therapeutic agent. In some embodiments, the second cancer therapeutic agent is a chemotherapeutic agent. In some embodiments, the pharmaceutical composition further comprises a second agent for treatment of cancer. In some embodiments, the second agent is a tumor vaccine. In some embodiments, an agent described herein may be conjointly administered with an additional agent. As used herein, the phrase "conjoint administration" refers to any form of administration of two or more different therapies (e.g., a therapy comprising an agent or composition) such that the second therapy is administered while the previously administered therapy is still effective in the body (e.g., the two compounds are simultaneously effective in the patient, which may include synergistic effects of the two compounds). Different therapies may be administered either in the same formulation or in separate formulations, either concomitantly or sequentially. In certain embodiments, the different therapies can be administered within one hour, 24 hours, 48 hours, a week, or one month of one another. Thus, an individual who receives such treatment can benefit from a combined effect of different therapies.

As described in detail below, the pharmaceutical compositions and/or agents disclosed herein may be specially formulated for administration in solid or liquid form, including those adapted for the following: (1) oral administration, for example, drenches (aqueous or non-aqueous solutions or suspensions), tablets, e.g., those targeted for buccal, sublingual, and systemic absorption, boluses, powders, granules, pastes for application to the tongue; or (2) parenteral administration, for example, by subcutaneous, intramuscular, intravenous, intrathecal, intracerebral or epidural injection as, for example, a sterile solution or suspension, or sustained-release formulation. Methods of preparing pharmaceutical formulations or compositions include the step of bringing into association an agent described herein with the carrier and, optionally, one or more accessory ingredients. In general, the formulations are prepared by uniformly and intimately bringing into association an agent described herein with liquid carriers, or finely divided solid carriers, or both, and then, if necessary, shaping the product.

Pharmaceutical compositions suitable for parenteral administration comprise one or more agents described herein in combination with one or more pharmaceutically-acceptable sterile isotonic aqueous or nonaqueous solutions, dispersions, suspensions or emulsions, or sterile powders which may be reconstituted into sterile injectable solutions or dispersions

just prior to use, which may contain sugars, alcohols, antioxidants, buffers, bacteriostats, solutes which render the formulation isotonic with the blood of the intended recipient or suspending or thickening agents.

Examples of suitable aqueous and nonaqueous carriers which may be employed in the pharmaceutical compositions include water, ethanol, dimethyl sulfoxide (DMSO), polyols (such as glycerol, propylene glycol, polyethylene glycol, and the like), and suitable mixtures thereof, vegetable oils, such as olive oil, and injectable organic esters, such as ethyl oleate. Proper fluidity can be maintained, for example, by the use of coating materials, such as lecithin, by the maintenance of the required particle size in the case of dispersions, and by the use of surfactants.

BRIEF DESCRIPTION OF FIGURES

Figure 1 includes 8 panels (Panels A-H). Panel A shows representative plots describing the sorting process of naïve $CD4^+$ T cell: (Ai) gating on the lymphocyte population based on forward-side scatter measures. (Aii) Exclude all cell aggregates. The three last steps use cell-surface markers, gating on cells that are: $CD25^{neg}$ (iii), $CD62L^{pos}$ (iv) and $CD44^{lo}$ (v). (Panel B) Glutamine uptake was measured by analyzing the growth media of $CD4^+$ T cells purified and activated as described in Figure 1A (n=4 pools of 4 mice each). (Panel C) Quantitation of the EM micrographs (Figure 2, Panel I) showed induction in cell area with T cell activation. (Panel D) Experimental scheme. Purified naïve $CD4^+$ T cells were either activated using plate-bound anti-CD3/anti-CD28, or maintained as 'resting cells' in the presence of IL-7 for assessment of mitochondrial respiration using the Seahorse Extracellular Flux Analyzer. (Panel Ei–Eii) Assessment of mitochondrial function by the Seahorse Extracellular Flux Analyzer: After measuring basal respiration, the cells were treated with oligomycin, an ATP synthase inhibitor, to assess ATP-coupled respiration and the extent of proton leak. The cells were then treated with an uncoupler (FCCP) to allow the free flow of protons back into the mitochondrial matrix, thus enabling mitochondrial respiration at maximal capacity. Finally, rotenone (complex I inhibitor) and antimycin-A (complex III inhibitor) were added to block mitochondrial respiration. Basal respiration (Panel F), and maximal respiratory capacity (Panel G) were calculated based on the changes in oxygen consumption rates, as described in panel F (n=5 pools of 2 mice each). (Panel H) Cellular ATP content was measured by a luminescence-based assay (n=5). *$p<0.05$, **$p<0.01$, ***$p<0.001$ (Student's t-test comparing activated vs. resting cells at each time

point (G,H); One-Way ANOVA followed by Tukey's multiple comparisons test, showing significant changes over naïve cells (Panels B-D, I). Results are mean ± SEM.

Figure 2 includes 16 panels (Panels A-P) showing naïve $CD4^+$ T cell stimulation initiates a synchronized program of mitochondrial biogenesis and activation. (Panel A) Scheme of experimental design. Purified naïve $CD4^+$ T cells were activated, and harvested at 0, 4, 9 and 24 hr post-activation as indicated. To verify proper cell activation, the cells were stained with cell surface markers, and analyzed by flow cytometry. Representative flow-cytometry plots (from >5 individual experiments) demonstrate: (Panel B) activation-induced growth in cell size, (Panel C) up-regulation of CD69 and CD25, and down regulation of the L-selectin CD62L. (Panel D) To assess proliferation, cells were stained with CellTrace Violet and analyzed by flow cytometry at 24, 48 and 72 hr post-activation. The representative FACS histograms demonstrate cell proliferation (detected by dilution of CellTrace Violet) occurring at 48 and 72 hr post-activation. (Panel E) Glucose uptake, and (Panel F) lactate secretion were measured by analyzing the growth media of $CD4^+$ T cells purified and activated as described in Figure 1A (n=4 pools of 4 mice each). (Panel G) Heatmap shows kinetic changes in metabolite levels in activated vs. naïve $CD4^+$ T cells. (Panel H) Representative 3D reconstructions of Z-stacks taken by live-cell imaging of activated $CD4^+$ T cells from $PHAM^{excised}$ mice. (Panel I) Representative EM micrographs of naïve $CD4^+$ T cells at 0, 4, 9 and 24 hr post-activation. Upper panel scale bar indicates 2 μm. Rectangle indicates region represented in lower panels, with a scale bar of 200 nm. Asterisk indicates orientation of panel. (Panels J-L) Quantitation of the EM micrographs (n=30 images per sample, 4-5 samples time point) showed changes over time in single mitochondrial area (Panel J), the % of cell area occupied by the mitochondria (Panle K) and the number of mitochondria per cell (Panel L). (Panel M) qPCR analysis of mitochondrial (*Cox-I*) vs. nuclear (*Rp18s*) DNA content (n=4 pools of 4 mice). (Panel N) Quantitation of mitochondrial length in EM micrographs. (Panel O) Oxygen consumption rate between resting and activated (24 hr) T cells. (Panel P) Spare respiratory capacity calculated based on the changes in oxygen consumption rates (n=5 pools of 2 mice each). $^{**}p<0.01$, $^{***}p<0.001$ (Student's t-test comparing activated vs. resting cells at each time point (P); One-Way ANOVA followed by Tukey's multiple comparisons test, showing significant changes over naïve cells. Results are mean ± SEM of 2-3 individual experiments.

Figure 3 includes 6 panels (Panels A-F) showing that quantitative proteomics identifies differential induction of metabolic pathways with naïve T cell activation. (Panel A)

Experimental scheme. Naïve $CD4^+$ T cells from two separate pools of mice were activated using plate-bound anti-CD3/anti-CD28, collected, and processed by protein extraction and digestion. The peptide pool from each of the 8 samples were labeled with a specific TMT label, equally mixed based on cell numbers and analyzed by LC-MS/MS, to yield protein quantitation. (Panel B) Scatter plots showing the biological replicates at 24 hr are well correlated. (Panel C) Graph demonstrating the overall induction in protein content during T cell activation. Values are the average of the two biological replicates at each time point. (Panel D) Heatmap showing the kinetics of changes in $CD4^+$ T cell proteomics following activation. (Panel E) 6 Representative clusters (see Figure S2 for clusters 7-12), of proteins that share similar expression kinetics with T cell activation. Kegg pathway analysis identified the specific metabolic pathways enriched within each cluster. (Panel F) A list of the proteins in cluster 1, representing the proteins with the greatest induction at 4 hr.

Figure 4 includes two panels (Panels A and B). (Panel A) Scatter plots of the proteomic dataset, showing the correlation between biological replicates at 4 and 9 hr post-activation. (Panel B) Clusters 7-12 of proteins that share similar expression kinetics during T cell activation (see Figure 3, Panel E for clusters 1-6).

Figure 5 includes 6 panels (Panels A-F) showing mitochondrial protein composition is changed with T cell activation. (Panel A) Histogram showing the kinetic distribution of mitochondrial proteome induction following $CD4^+$ T cell activation. Color codes show in blue: proteins induced more than one standard deviation below mean distribution, in red: proteins induced more than one standard deviation above mean distribution, and in grey: proteins induced within mean distribution. Values are the average of the two biological replicates at each time point. (Panel B) Heatmap summarizing the results of a GSEA analysis of the mitochondrial proteome indicating in blue, pathways that were significantly downregulated by 24 hr post-activation, and in red: pathways that were significantly upregulated by 24 hr post-activation. The analysis was performed on the full list of mitochondrial proteins, pre-ranked based on their fold-change induction compared to naïve T cells. Yellow asterisk indicates $P<0.05$. (Panel C) The mitochondrial proteome was segregated into 4 clusters based on protein level kinetics following T cell activation. Kegg pathway analysis identified the specific metabolic pathways enriched within each cluster. (Panel D) Graph showing fold-change induction of individual proteins in pathways of one carbon metabolism, TCA cycle, fatty acid oxidation 24 hr post-activation. Electron transport chain complexes are shown as the average level of individual subunits within each complex.

Values are the average of two biological replicates, normalized to porin (Panel E) Graph showing the average induction of mitochondrial metabolic pathways from panel D compared to porin. (Panel F) Schematic of central metabolic pathways in the mitochondria. In all panels *p<0.05, **p<0.01 (Student's t-test comparing each of the metabolic pathways to porin). Results are mean ± SEM.

Figure 6 shows the Western blot analysis of metabolic enzymes in naïve T cells versus T cells at 24 hr post-activation. Porin and actin were loading controls for each blot.

Figure 7 includes 7 panels (Panels A-G) showing the enzymes involved in one carbon metabolism and pyrimidine biosynthesis are induced in-vivo on antigen specific T cells, following immunization. (Panel A) Schematic showing central metabolic pathways in the mitochondria, listing representative enzymes, color-coded based on their fold-change at 24 hr post-activation. In blue: proteins induced more than one standard deviation below mean distribution, in red: proteins induced more than one standard deviation above mean distribution, and in grey: proteins induced within mean distribution. (Panel B) Protein quantitation by western blot of the enzymes listed in (Panel A) using porin and β-actin as loading controls. See Figure 6 for the complete set of controls for individual proteins. (Panel C) Experimental strategy. Naïve, mog-specific $CD4^+$ T cells were isolated from 2D2 TCR transgenic (Tg) mice and transferred into C57Bl/6 wild-type recipients, in conjugation with mog/CFA immunization. Mice (n=4 per timepoint) were sacrificed at days 2, 3 and 4 following immunization for analysis of the T cells in the draining lymph nodes by flow cytometry. (Panel D) Representative plots showing the accumulation of Tg mog-specific T cells TCRβ11/ TCRα3.2 in the draining lymph nodes following immunization. (Panel E) Immunization generated a specific anti-mog immune response. Graph showing the % of proliferating cells ($Ki67^+$), comparing mog-specific T cells to the non-specific host T cell population. *p<0.05, ***p<0.001 (Student's t-test comparing wild-type and mog-specific T cells at each time point). (Panel F) Representative plots showing the kinetics of CD69 expression on mog-specific T cells following immunization. (Panel G) Representative plots showing changes in cell size (FSC), and expression of metabolic enzymes on mog-specific T cells following immunization. N=4 mice per time point in each experiment. Entire experiment was performed 2-3 times. Results are mean ± SEM.

Figure 8 includes 7 panels (Panels A-G) showing mitochondrial one-carbon metabolism is induced in $CD4^+$ T cells upon activation, and contributes to de-novo purine biosynthesis. (Panel A) Schematic showing major metabolic pathways contributing to purine

biosynthesis. αPRPP – phosphoribosyl pyrophosphate; AICAR- 5-Aminoimidazole carboxamide ribonucleotide; IMP – inosine monophosphate; XMP-xanthosine monophosphate; GMP – guanosine monophosphate; AMP-adenosine monophosphate. (Panel B) Heatmap showing Log2 fold-change of intermediates in purine biosynthetic pathways, in activated compared to naïve T cells, measured by LC-MS. (Panel C) Graph summarizes changes in culture media composition from naïve, 4, 9 and 24 hr post-activation, highlighting lactate secretion (red) and hypoxanthine consumption (blue). (Panel D) Schematic of the metabolic tracing of the one carbon metabolic pathway using uniformly labeled $^{13}C_3$-serine, highlighting the incorporation of its products: glycine ($^{13}C_2$) and two molecules of 10-formyl-THF ($^{13}C_1$) into the purine ring, thru de-novo purine biosynthesis. THF- tetrahydrofolate. (Panel E) ^{13}C labeling of representative purine molecules IMP, ADP and GDP shows increased % labeling over time, confirming that one-carbon metabolism is induced by T cell activation. (Panel F) Metabolic tracing strategy using uniformly labeled D_3-serine, to differentiate flux thru the mitochondrial versus the cytosolic arm of one-carbon metabolism by monitoring the labeling pattern of thymidylate. DHF-dehydrofolate (Panel G) Activated T cells produce predominantly the m+1 isotopomer of dTMP and dTTP, indicative of mitochondrial rather than cytosolic flux.

Figure 9 includes 5 panels (Panels A-E) showing that ^{13}C labeling of purine molecules shows increased labeling over time, confirming that one carbon metabolism is induced by T cell activation.

Figure 10 includes 11 panels (Panels A-K) showing genetic inhibition of mitochondrial one-carbon metabolism impairs T cell survival ex vivo and in vivo. (Panel A) Schematic shows the enzymes involved in mitochondrial and cytosolic branches of one-carbon metabolism. SHMT: Serine hydroxymethyltransferase; MTHFD: methylenetetrahydrofolate dehydrogenase; MTHFD1L: methylenetetrahydrofolate dehydrogenase 1-like. (Panel B) Protein quantitation of SHMT2 in non-infected cells (WT) or cells infected with retrovirus containing 2-3 individual shRNA sequences against LacZ (control) or SHMT2. (Panel C) Resting $CD4^+$ T cells infected with either sh-LacZ (control, sh-1) or sh-SHMT2 (sh-1, sh-3) were re-activated in media containing only D3-serine for 48 hr, and analyzed by LC-MS. Knockdown of SHMT2 increased the relative abundance of the m+2 over the m+1 dTTP isotopomer, indicative of an increased cytosolic one carbon metabolism when the mitochondrial arm is inhibited. (Panel D) Resting $CD4^+$ T cells infected with either sh-LacZ (control, sh-1) or sh-SHMT2 (sh-1, sh-3) were re-activated for

48 hr and analyzed by LC-MS. Cells with reduced SHMT2 levels showed accumulation of metabolites in de-novo purine biosynthesis that precede the incorporation of the one-carbon unit 10-formyl THF. (Panel E) Representative plots showing normal levels of activation markers (CD69 and CD25) on SHMT2 knockdown cells. (Panels F-H) To assess cell proliferation, resting $CD4^+$ T cells infected with either sh-LacZ (control sh-1) or sh-SHMT2 (sh-1, sh-3) were stained with CellTrace Violet, and analyzed by flow cytometry 48 hr post-activation. (Panel F) Representative histogram of cell proliferation. (Panel G) Representative plots showing proliferation vs. cell death (measured by 7-AAD incorporation), and (Panel H) % dead cells ($7\text{-}AAD^+$). (Panel I) Experiment strategy. C57Bl/6J mice were injected with resting $CD4^+$, mog-specific T cells infected with retrovirus expressing GFP^+ sh-control or GFP^+ sh-SHMT2 and immunized with mog/CFA. 5 days post-immunization, the mice were sacrificed and the draining lymph nodes analyzed by flow-cytometry for GFP^+ cells. (Panel J) % GFP^+ cells out of total $CD4^+$ T cells, in the immunized mice. (Panel K) To assess cell proliferation, cells from the draining lymph nodes were stained for Ki67. Graph shows % $Ki67^+$ cells out of infected (GFP^+) $CD4^+$ T cells. Experiment was performed two times with n=7 mice per group for each experiment. $^{**}p<0.01$, $^{***}p<0.001$ (Student's t-test (Panels I and J); One-Way ANOVA followed by Tukey's multiple comparisons test, showing significant changes over sh-control cell (Panel G). Results are mean ± SEM

Figure 11 includes 8 panels (Panels A-H) (Panel A) Experimental scheme for retroviral infection and re-activation of $CD4^+$ T cells. Naïve $CD4^+$ T cells were activated with low concentrations of plate-bound anti-CD3/anti-CD28. 24 hr post-activation, the cells were collected and spin-fected with GFP-labeled retrovirus, followed by 2 days of incubation with IL-2 and 2 days incubation with IL-7. The infected resting, T cells were then collected, sorted for GFP^+ T cells (infected), reactivated using a higher dose of plate-bound anti-CD3/anti-CD28, and analyzed as described. (Panel B) Representative flow cytometry plots of resting and re-activated $CD4^+$ T cells demonstrate cell growth and activation marker expression (CD69 upregulation, CD25 upregulation and CD62L downregulation) in the reactivated cells. (Panel C) To assess proliferation, the cells were loaded with CellTrace Violet, and analyzed by flow cytometry at 48 and 72 hr post-reactivation. The representative flow cytometry histograms demonstrate cell proliferation (detected by dilution of CellTrace Violet) occurring at 48 and 72 hr post-reactivation. (Panel D) qPCR analysis of mitochondrial (*Cox-I*) vs. nuclear (*Rp18s*) DNA content in resting and reactivated cells. (Panel E) Representative Western blots showing SHMT2 induction in reactivated compared

to resting T cells. (Panels F-G) To assess cell proliferation, resting $CD4^+$ T cells infected with either sh-SHMT2 or sh-control were loaded with CellTrace Violet, and dye dilution analyzed by flow cytometry at 72 hr post-activation (Panel F) Representative histogram of cell proliferation. (Panel G) Representative plots showing proliferation vs. Cell death (measured by 7-AAD incorporation) (Panel H) % dead cells ($7\text{-}AAD^+$) at 72 hr post-activation. All experiments were performed 2-3 times.

Figure 12 is a bar graph showing a combination of n-acetyl cysteine (NAC) and nicotinamide mononucleotide (NMN) rescues cell death of SHMT2 KD T cells

Figure 13 shows an exemplary amino acid sequence for a wild type human SHMT1.

Figure 14 shows an exemplary amino acid sequence for a wild type human SHMT2.

Figure 15 shows an exemplary amino acid sequence for a wild type human MTHFD1.

Figure 16 shows an exemplary amino acid sequence for a wild type human MTHFD2.

Figure 17 shows an exemplary amino acid sequence for a wild type human MTHFD1L.

Figure 18 shows an exemplary amino acid sequence for a wild type human MTHFD2L.

Figure 19 shows KD of SHMT2 causes nucleotide imbalance and increased oxidative burden, leading to increased accumulation of DNA damage and increased cell death. These phenotypes are reversed by supplementation with formate and anti-oxidants (NAC). Here, it is shown that knockdown of SHMT2 causes nucleotide imbalance, with an overall reduction in purine levels, and normal levels of pyrimidines (Panel A). Such nucleotide imbalance can cause DNA damage. Indeed, SHMT2 KD T cells accumulate γ-H2A.X, an indicator of DNA damage (Panel B). In addition, it was found that a blockade in mitochondrial on-carbon metabolism cause by KD of SHMT2 caused a reduction in total glutathione levels (Panel C). Finally, it is shown that supplementation with the glutathione precursor, NAC, in combination with formate, the one-carbon unit generated in the mitochondria and used for purine biosynthesis, is sufficient to rescue cell death in the SHMT2 KD cells (Panel D).

Figure 20 shows SHMT2 is suppressed in tumor infiltrating T cells. Bulk $CD45^+CD3^+CD8^+$ T cells were sorted from the draining lymph nodes or tumors of MC38-bearing wild-type mice. The Cre^+ mice clear tumors after about 15 days, and this experiment

was harvested on day 10. $CD8^+$ T cells were sorted from tumors and draining lymph nodes and used for analysis by RNAseq. RNAseq dataset was used to assess the effect of the tumor microenvironment on expression of genes in the 1C metabolic pathway that were highly induced in our proteomic dataset of T cell activation (The genes tested were: SHMT1, SHMT2, MTHFD1, MTHFD1L, MTHFD2, MTHFD2L, FPGS, TYMS, DHFR, MTHFS, MTRR). We identified a specific downregulation of SHMT2 in tumor infiltrating $CD8^+$ T cells compared to T cells in the draining lymph nodes. Previous studies identified SHMT2 as a critical metabolic enzyme important for T cell proliferation and survival. These RNAseq data suggest suppression of SHMT2 as a potential novel mechanism of T cell suppression in the tumor microenvironment.

Figure 21 shows T cells from aged mice exhibit impaired activation of naïve $CD4^+$ T cells. CD4+ T cells were isolated from the spleens of young (2 mo. old) and aged (20 mo. old) mice by magnetic separation, and sorted by flow cytometry to yield rigorously naïve T cells. Cells were activated by plate-bound anti-CD3/anti-CD28 and harvested at 24 and 48 hr post-activation (Panel A). Activation induced cell growth was analyzed by flow-cytometry, and demonstrated that activation-induced growth was diminished in aged mice (Panel B). To assess proliferation, cells were stained with CellTrace Violet prior to activation, and analyzed by flow cytometry at 48 hr post-activation. Proliferation of aged CD4+ T cells was impaired, indicated by increased non-proliferating cells (generation 0) and reduced proliferating cells (generation 2) (Panel C). T assess cell viability, we analyzed 7-AAD incorporation, and found a significant induction of cell death in the aged T cells.

Figure 22 shows activation-induced upregulation of one-carbon metabolism is blunted in T cells from aged mice. Quantitative multiplex proteomics to show that activation of young $CD4^+$ T cells induces mitochondrial proteome remodeling to stimulate one-carbon metabolism. A similar approach was taken and multiplex proteomics was performed on young versus aged $CD4^+$ T cells to quantify expression of 3500 proteins during T cell activation. This new dataset shows a specific deficiency in the induction of proteins in one-carbon metabolism in aged T cells compared to the induction of proteins in other pathways, such as fat metabolism, TCA cycle, or respiration. The graph shows ratio of fold-change induction in protein levels of metabolic enzymes in central mitochondrial pathways in aged vs. young $CD4^+$ T cells. These results suggest that defective induction of one-carbon metabolism during aging leads to increased cell death and impaired immune function.

Figure 23 shows addition of formate to growth media improves activation-induced cell growth in T cells from aged mice. To test whether aged T cell phenotypes could be rescued through metabolic intervention, T cells were treated with formate, the one-carbon unit generated through mitochondrial one-carbon metabolism, shown to rescue SHMT2 KD T cells. Naïve aged T cells were activated ex-vivo in control media or media supplemented with 1mM formate. The cells were harvested at 24 hr post-activation and analyzed by flow cytometry to assess cell growth (Panel A). Addition of these metabolites increased activation-induced cell growth (Panel B, Panel C). These experiments provide a proof of concept that metabolic intervention can alleviate aspects of T cell aging.

EXAMPLES

Experimental procedures

Mice

The mice used for all experiments were 7-10 weeks old. Wild-type C57BL/6 and C57Bl/6-Tg(Tcra2D2,Tcrb2D2)1Kuch mice were purchased from the Jackson Laboratory (Bar Harbor, ME). PhAM^{excised} mice were the generous gift of Dr. David Chan. Experimental mice were housed in specific pathogen-free conditions at Harvard Medical School and used in accordance with animal care guidelines from the Harvard Medical School Standing Committee on Animals and the National Institutes of Health.

Culture and stimulation of naïve CD4$^+$ T cells

Sorted naïve CD4$^+$ T cells were cultured at 37°C and 5% CO_2 in complete RPMI media (RPMI, supplemented with 10% FCS, 10 mM HEPES, 10 U/ml penicillin/streptomycin, and 50 μM β-mercaptoethanol (all from Life Technologies)), and activated *in vitro* with 4 μg/mL plate-bound anti-CD3 (clone 1H5-2C11; BioXCell) and anti-CD28 (clone 37.51; BioXCell). In some experiments, IL-7 (5 ng/mL; R&D Systems), or formate (1mM; SIGMA) were added to culture media. For retroviral transduction, naïve CD4$^+$ T cells were stimulated for 24h with plate bound anti-CD3 (1 μg/ml) and anti-CD28 (0.5 μg/ml) in complete RPMI media, supplemented with 100 μM non-essential amino acids (GIBCO), 1 mM sodium pyruvate (GIBCO) and recombinant IL-2 (100U/mL; Peprotech).

Adoptive transfer & Immunization

Naïve CD4$^+$ T cells were isolated from TCR-transgenic 2D2 (Mog-specific) mice, and transferred by tail-vein injection into WT recipients (1-2e^6 cells per mouse). In some experiments, the cells were retrovirally infected prior to adoptive transfer.

For MOG 35–55 immunizations (referred to as "MOG/CFA"), mice were injected

subcutaneously with 100μg of MOG 35–55 (UCLA Biopolymers Facility) emulsified in a 1:1 emulsion of H37RA CFA (Sigma) on the mouse flanks. At different time points (as indicated), the mice were euthanized and inguinal lymph nodes (dLN) were harvested for flow cytometric analyses.

Flow cytometry

In-vitro cultured cells, or cells isolated from lymphoid organs of immunized mice were collected, resuspended in staining buffer (PBS containing 1% fetal bovine serum and 2 mM EDTA), and stained directly with labeled antibodies from Biolegend against CD4 (RM4-5), CD25 (PC61), and CD69 (H1.2F3). For metabolic enzyme staining, the following antibodies were used: from Abcam: CPS1 (ab3682), from Proteintech: Dhodh (14877-1-AP), MTHFD1 (10794-1-AP), MTHFD2 (12270-1-AP), from Novus Biological: UMPS(NBP1-85895), SHMT1(NBP1-32173), Mthfs (NBP1-56698) followed by donkey-anti rabbit (Biolegend). For intracellular staining, the FoxP3 fix/perm kit (eBioscience) was used after surface staining. All flow cytometry was analyzed with an LSR II (BD biosciences) using standard filter sets, and were analyzed with FlowJo software (TreeStar).

Electron Microscopy: sample preparation, data collection and analysis

T cells were fixed with 0.1 M cacodylate buffer, pH 7.4, containing 2% glutaraldehyde, 2% paraformaldehyde, and mixed with 4% low melting-point agarose. The agarose blocks were washed with 0.1 M cacodylate buffer and post-fixed in 0.1 M cacodylate buffer containing 1% Osmium Tetroxide. Following washing with deionized water, the T cells were immersed in 2% aqueous uranyl acetate for contrast fixation overnight. Samples were washed with deionized water, followed by immersion in ethanol solutions and propylene oxide, for dehydration. Samples were rotated overnight in a 1:1 solution of propylene oxide and LX112 Epon resin, followed by an overnight incubation with 100% freshly made resin. The samples were then placed in a vacuum oven at 60 °C for 2 hr, embedded in BEEM capsules, and cured over 48 hr at 60°C. Cured blocks were sectioned using a Leica Ultracut E ultramicrotome. Sections were put on formvar-coated grids that had been carbon coated and glow discharged. Grids were contrast stained with 2% uranyl acetate and lead citrate. Imaging was done using a 1400 TEM (JEOL) equipped with a side mount Gatan Orius SC1000 digital camera at a nominal magnification of 20K (naïve, 4 and 9 hr) or 12K (24 hr). Micrographs were analyzed using Volocity 3D image analysis software (PerkinElmer).

Live cell imaging

Naïve $CD4^+$ T cells derived from PHAMexcised mice were activated in a 6 well plate on 25 mm round glass coverslips (Warner Instruments) pre-coated with anti-CD3/anti-CD28. At the desired time points, the coverslips were placed in a Attofluor cell chamber (Invitrogen) for imaging. Confocal microscopy was performed using a Mariana system (Intelligent Imaging Innovations, 3I) composed of an inverted, fully motorized Axio Observer microscope (Carl Zeiss Microimaging, Inc.) equipped with a cooled electron multiplication CCD camera with 512 × 512 pixels (QuantEM, Photometics) and a CSU-X1 spinning disc (Yokogawa Electric) upgraded with a Borealis illumination system equipped with a solid state 488 nm (Coherent) laser and 525/50 emission filter (Semrock). Live-cell 3D image stacks were obtained along the z axis using the 100× oil immersion 1.4 NA DIC objective moved with a piezo-based stage (Applied Scientific Instrumentation) by acquiring sequential optical planes imaged with 40 ms exposure and spaced 0.13 μm apart. 3D reconstruction was done using IMARIS (Bitplane).

Real-time PCR

Total DNA was isolated using DNeasy kit (Qiagen). cDNA was synthesized using the iSCRIPT kit (BioRad). Quantitative PCR analysis was performed with SYBR green, using a LightCycler 480 (Roche). Rp18s: F: 5'-ACCTGTCTTGATAACTGCCCGTGT-3', R: 5'-TAATGGCAGTGATGGCGAAGGCTA-3'; Cox1: F: 5'-ACTTGCAACCCTACACGGAGGTAA-3', R: 5'-TCGTGAAGCACGATGTCAAGGGAT-3'.

Measurement of intracellular ATP content

ATP content was measured from 0.8-1.5 x 10^6 cells per sample using the ATP colorimetric/fluorimetric Assay kit (Biovision), following the manufacturer's protocol. Results were normalized to cell numbers.

Proteomics data analysis

Fold change data was Lowess corrected and collapsed into unique protein representation to (average fold change of all peptides). The sorted heatmap of the log2 fold-changes was generated using SPIN. Proteins were clustered using the Agglomerative Clustering function from the SciKit-Learn machinelearning library in Python (scikit-learn.org). Data points used in clustering were a protein's abundance relative to naive T cells at 4, 9, and 24 hr following activation, in each of two experimental replicates (so that six data points per protein were used for clustering). Values from the two replicates were

averaged for drawing the curves in Figures 2 and 3. All proteins with at least 2 detected peptides were included in this analysis. The Molecular Signatures Database (MSigDB, Broad Institute; http://software.broadinstitute.org/gsea/msigdb/annotate.jsp) was used for Kegg pathway analysis. For mitochondrial proteins, each sample was z-scored normalized (average of 0 and standard deviation of 1), for gene set enrichment analysis (Broad Institute; http://software.broadinstitute.org/gsea/index.jsp).

Statistical analysis

All statistical analyses were performed using Prism (Graphpad Software). We used unpaired Student's t-test when comparing two groups, and one-way analysis of variance (ANOVA) followed by Tukey-Kramer's post hoc analysis, when comparing 3 groups.

Isolation of naïve $CD4^+$ T cells

To isolate naïve $CD4^+$ T cells, spleens were harvested, and single cell suspensions prepared by manual disruption and passage through a 70 μm cell strainer. Cells were washed and resuspended in PBS containing 1% fetal calf serum (FCS) and 2 mM EDTA, and bulk $CD4^+$ cells were purified by magnetic bead separation using anti-CD4 microbeads (Miltenyi Biotec). Cells were then stained with anti-CD25-FITC (clone PC61), anti-CD62L-PE (clone MEL-14) and anti-CD44-APC (clone IM7; all from BioLegend), and naïve cells ($CD25^-$ $CD62L^{hi}CD44^{lo}$) were purified by fluorescence-activated cell sorting using a MoFlo high-speed cell sorter (Beckman Coulter Life Sciences). Purity was confirmed by flow cytometric analysis prior to use of cells in experiments; in all cases, the sorted naïve cell population consisted of greater than 99% $CD25^-CD62L^{hi}CD44^{lo}$ cells.

Gene silencing by retroviral transduction

The pMKO.1 GFP retroviral vector (Addgene plasmid 10676) and pCL-Eco (Addgene plasmid 12371) were kindly provided by Prof. Bill Hahn (Harvard). Double strand oligonucleotides for short hairpin RNA (shRNA) against Shmt2 and Lacz were cloned into pMKO.1 GFP between AgeI and EcoRI sites. The sequences for Shmt2 shRNA are: Sh1 5'-CCGGCCTCATTGACTATGCACGCATCTCGAGATGCGTGCATAGTCAATGAGGTTTTTG-3' (sense strand) and 5'-AATTCAAAAACCTCATTGACTATGCACGCATCTCGAGATGCGTGCATAGTCAATGAGG-3' (antisense strand); Sh3 5'-CCGGCCGAATCAACTTCGCTGTGTTCTCGAGAACACAGCGAAGTTGATTCGGTTTTTG-3' (sense strand) and 5'-AATTCAAAAACCGAATCAACTTCGCTGTGTTCTCGAGAACACAGCGAAGTTGAT

TCGG-3' (antisense strand). The sequences for Lacz shRNA (control sh-1) are: 5'-CCGGCCGTCATAGCGATAACGAGTTCTCGAGAACTCGTTATCGCTATGACGGTTTTTG-3' (sense strand) and 5'-AATTCAAAAACCGTCATAGCGATAACGAGTTCTCGAGAACTCGTTATCGCTATGACGG-3' (antisense strand). Recombinant retrovirus was made by cotransfection of pMKO.1 GFP and pCL-Eco into 293T cells using Fugene 6 (Promega). Culture supernatants were collected 48 h after transfection. T cells were spinfected at 37 °C and 1900 rpm for 90 min with freshly collected retrovirus containing polybrene (8 μg/ml; SIGMA).

Protein content analysis by Western blot

Cells were lysed in lysis buffer (150mM NaCl, 50mM Tris-HCl, ph 7.5 and 0.5% NP-40) supplemented with protease inhibitor cocktail (Roche, South San Francisco, CA, USA). Lysates were mixed with sample buffer (4× Tris. Cl/ SDS, pH 6.8, 30% glycerol, 10% SDS, 0,6 M DTT, 0.012% bromophenol blue) under reducing conditions, were separated by sodium dodecyl sulfate polyacrylamide gel electrophoresis, and transferred to nitrocellulose membranes. The membranes were incubated for 1 hr in Tris-Buffered Solution (TBS) containing 0.1% Tween 20 and 5% nonfat milk, followed by an overnight incubation with the respective primary antibodies at 4 °C. The membranes were then washed and incubated with horseradish peroxidase-conjugated secondary antibody for 1 hr, washed and developed using an enhanced chemiluminescence reagent (Thermo Scientific). The list of primary antibodies used: From Proteintech: Cpt1a, Mthfd1, Mthfd2, Dhodh, Asl. From Novus Biologicals: Shmt1, Umps. From abcam: Shmt2, Ogdh. From Cell Signaling: Acc1, Mdh2. From Santa Cruz: Odc, Otc. From Sigma: Actin.

Mitochondrial respiration

Oxygen consumption rates (OCR) were measured from cells in non-buffered DMEM containing 5 mM glucose, 2 mM L-glutamine, and 1 mM sodium pyruvate, under basal conditions and in response to mitochondrial inhibitors: 5 μM oligomycin, 1 μM FCCP, 100 nM rotenone, and 1 μM antimycin A (All from Sigma) on the XF-24 Extracellular Flux Analyzer (Seahorse Bioscience).

Metabolomics and metabolite uptake and tracing

Glucose and glutamine uptake, and lactate secretion were measured by analyzing growth media using the BioProfile Flex Analyzer (Nova Biomedical). For carbon and deuterium tracing, and non-labeled metabolomics, $CD4^+$ T cells were collected and filtered using a borosilicate glass fritted support base (Corning) and a 0.45μm nylon membrane

(Millipore), followed by washing with 1mL PBS. The membranes were then immediately submerged in 1mL cold 80% MeOH. Total time from perturbation of the cells to quenching was < 1 min. The quenched filter was incubated in -80°c for 15 min, flipped over and incubated for another 15 min. The supernatants were collected and centrifuged: 17,000g, 5 min at 4°c. Following centrifugation, the supernatants were collected and dried by SpeedVac. For analysis of metabolite content in culture media, 50 µl of media was added to a tube containing 200 µl dry-ice cold MeOH, vortexed, and incubated on dry ice for 30 min, following by centrifugation (17,000g, 5 min at 4°C) and dilution in HPLC-grade water. For analysis of metabolite content by mass spectrometry, the intracellular supernatants were dried and resuspended in 80µl of HPLC-grade water. Samples were analyzed by reversed-phase ion-pairing chromatography coupled with negative-mode electrospray-ionization high-resolution MS on a stand-alone orbitrap (Thermo). Data were analyzed using the MAVEN software suite. Metabolite abundance was normalized to cell count. Carbon isotope labeling patterns were corrected for ^{13}C natural abundance and impurity of labeled substrate. ^{2}H isotope labeling was corrected for ^{18}O, ^{13}C and ^{15}N natural abundance for high molecular weight species that could not be individually resolved (>250 Da). Correction was done by least squares (NNLS package in R) fitting of the following equation and solving for the deuterium labeling vector, D_0, D_1, D_i:

$$\begin{bmatrix} (0,n,N_x) & 0\ldots & 0\ldots. \\ (1,n,N_x) & (0,n,N_x) & 0\ldots. \\ (i,n,N_x) & (1,n,N_x) & (0,n,N_x) \end{bmatrix} \times \begin{bmatrix} Isotope\ y \end{bmatrix} \times \begin{bmatrix} Isotope\ z \end{bmatrix} \times \begin{bmatrix} D_0 \\ D_1 \\ D_i \end{bmatrix} = \begin{bmatrix} M \\ M+1 \\ M+i \end{bmatrix}$$

$$(i,n,N_x) = \binom{n}{i} (N_x)^i (N_x)^{n-i}$$

Where n = number of potentially labeled atoms of isotope x, i= the i^{th} potentially labeled atom, N_x is the natural abundances of isotope x, and M, $M+1$, $M+i$ is the measured isotopic labeling distribution.

Protein extraction for mass spectrometry

Cell pellets were mixed in 200 µl lysis buffer (2% SDS, 150mM NaCl, 50mM Tris (pH 8.5), proteinase inhibitor mix, 5mM DTT) and incubated on ice for 10 min, followed by incubation in 60°c for 45 min. Samples were allowed to cool back to room temperature, mixed with iodoacetamide to a final concentration of 14 mM, and incubated for 45 min at room temperature. Samples were then mixed with 3 parts ice-cold methanol, 1 part chloroform and 2.5 parts H_2O, and centrifuged at 4000g for 10 min. Following removal of

the top layer, 3 parts of ice-cold methanol were added, followed by centrifugation at 4000g for 5 min. Following removal of the top layer, the samples were mixed with 3 parts of ice-cold acetone, vortexed, and centrifuged at 4000g for 5 min. The pellet was then washed one more time in 2 mL ice-cold acetone, and stored at (-80°C) prior to enzymatic digestion.

Enzymatic digestion for mass spectrometry

Protein pellets from equal cell equivalents were resuspended in 4 M urea, 75 mM NaCl, 50 mM Tris-Cl pH 8.8. Samples were then diluted to 1 M urea with 50 mM Tris-Cl pH = 8.8 and lysyl endopeptidase (lysC, Wako Chemicals USA, Inc.) was added at 1:50 (wt:wt) enzyme:substrate. After 6 hours at room temperature, trypsin (Promega) was added at the same ratio and digestion was allowed to proceed overnight at 37°C. Digests were acidified by the addition of 100% formic acid (FA) to 2% final concentration and the peptides were desalted on 50 mg tC18 Sep-Pak cartridges (Waters) and dried in a centrifugal evaporator.

TMT-labeling

Peptides were resuspended in 100 µl of 0.2 M Hepes buffer, pH 8.5. TMT8plex amino reactive reagents (0.8 mg per vial) (Thermo Fisher Scientific) were resuspended in 40 µl of anhydrous acetonitrile (ACN) and 10 µl of each reagent was added to each sample and mixed briefly on a vortex. Reactions were allowed to proceed at room temperature for 1 hr, and then quenched by the addition of 8 µl of 5% hydroxylamine for 15 min and then acidified by the addition of 16 µl 100% FA. Reaction products from all eight differentially labeled samples were combined and 1 ml of 1% FA was added before desalting on a 200-mg tC18 Sep-Pak. Eluted peptides were dried and stored at −20°C.

Peptide fractionation

TMT-labeled peptides were resuspended in 250 □l buffer A (5% ACN, 10 mM NH4HCO3, pH 8) and separated by high-pH reverse-phase HPLC on a 4.6 mm × 250 mm 300Extend-C18, 5 µm column (Agilent) using a 50 min gradient from 18% to 38% buffer B (90% ACN, 10 mM NH4HCO3, pH 8) at a flow rate of 0.8 ml/min. Fractions were collected over 45 min at 28 s intervals beginning 5 min after the start of the gradient in a 96-well plate and lyophilized. Fractions were resuspended in 30 µl 1% FA and combined by pooling eight fractions down each plate column, such that pool 1 = 1/13/25/37/49/61/73/85, pool 2 = 2/14/26/38/50/62/74/86, etc. The pooled samples were desalted on hand-packed C18 STAGE Tips, eluted into glass vial inserts and resuspended in 20 µl of 5% FA.

LC-MS/MS analysis

For TMT experiments, 5 µl of each fraction was analyzed on a Thermo Orbitrap Fusion mass spectrometer (Thermo Fisher Scientific) equipped with an Easy nLC-1000 UHPLC (Thermo Fisher Scientific). Peptides were separated with a gradient of 6–24% ACN in 0.125% FA over 150 min and introduced into the mass spectrometer by nano-electrospray as they eluted off a self-packed 18 cm, 100 µm (ID) reverse-phase column packed with 3 µm, 200 Å pore size, Maccel C18 AQ resin (The Nest Group, Southborough, MA). They were detected using a data-dependent Top10-MS^2/MS^3, 'multi-notch' method. For each cycle, one full MS scan was acquired in the Orbitrap at a resolution of 120,000 with automatic gain control (AGC) target of 2×10^5. Each full scan was followed by the selection of the most intense ions, up to 10, for collision-induced dissociation (CID) and MS^2 analysis in the linear ion trap for peptide identification using an AGC target of $4x10^3$ and a maximum ion accumulation time of 150 ms. Ions selected for MS^2 analysis were excluded from reanalysis for 60 s. Ions with +1 or unassigned charge were also excluded from analysis. A single MS^3 scan was performed for each MS^2 scan selecting up to the 10 most intense ions from the MS^2 for fragmentation in the HCD cell using an AGC of $5x10^4$ and max accumulation time of 150 ms. The resultant fragment ions were detected in the orbitrap at a resolution of 60000.

Database searching and filtering

MS^2 spectra were matched to peptide sequences using SEQUEST v.28 (rev. 13) and a composite database containing the translated sequences of all predicted mouse open reading frames (Uniprot, downloaded 8/10/2011) and its reversed complement. Search parameters allowed for two missed cleavages, a mass tolerance of 20 ppm, static modifications of 57.02146 Da (carboxyamidomethylation) on cysteine and 229.16293 Da (TMT label) on peptide amino termini and lysines, and a dynamic modification of 15.99491 Da (oxidation) on methionine. Peptide spectral matches were filtered to 1% false discovery rate (FDR) using the target-decoy strategy combined with linear discriminant analysis (LDA) using the SEQUEST Xcorr and ΔCn' scores, precursor mass error, observed ion charge state, and the number of missed cleavages. LDA models were calculated for each LC-MS/MS run with peptide matches to forward and reversed protein sequences as positive and negative training data. The data were further filtered to control protein-level FDRs. Protein scores were derived from the product of all LDA peptide probabilities, sorted by rank, and filtered to 1% FDR. The FDR of the remaining peptides fell markedly after protein filtering. Further filtering based on the quality of quantitative measurements (see below) resulted in a final

protein FDR < 1% for all experiments. Remaining peptide matches to the decoy database as well as contaminating proteins (e.g., human keratins) were removed from the final data set.

Peptide and protein quantification

For TMT experiments reporter ion signal-to-noise values were extracted and corrected for isotopic overlap between reporter ions by using empirically derived values. We required each peptide to have sum sn ≥ 300 and no more than two zero values for any of the eight TMT channels. Protein ratios were calculated as the weighted average of all peptides from each protein using the ratio of the summed reporter ion intensities in each channel. Ratios were log2-transformed for all subsequent analysis.

Example 1 - Naïve $CD4^+$ T cell stimulation initiates a synchronized program of mitochondrial biogenesis and activation.

To probe the contribution of mitochondria to T cell activation, a well-established system for in vitro activation of purified, sorted naïve $CD4^+$ T cells was utilized (Figure 1, Panel A). Naïve $CD62L^{hi}CD44^{lo}CD25^-$ $CD4^+$ T cells were stimulated ex vivo using a combination of anti-CD3/anti-CD28 antibodies to mimic the T cell receptor-mediated signal and the CD28 costimulatory signal, respectively (Figure 2, Panel A). Activation of T cells using these conditions led to an increase in cell size (Figure 2, Panel B), upregulation of the early activation markers CD69 and CD25, and downregulation of L-selectin (CD62L), compared to naïve $CD4^+$ T cells at 24 hours post-stimulation (Figure 2, Panel C). To assess the kinetics of T cell division under these conditions, naïve $CD4^+$ T cells were labelled with CellTrace violet, and analyzed dye dilution (as an indication of cell division) by flow cytometry at 24, 48 and 72 hr following activation. Proliferation occurred only at 48 and 72 hr post-activation (Figure 2, Panel D). As anticipated, outputs of metabolic activation in T cells, such as glucose and glutamine uptake and lactate secretion were significantly increased (Figure 2 Panel E, Figure 1, Panel B, and Figure 2, Panel F, respectively). In addition, mass spectrometry was utilized to measure the levels of intermediates of glycolysis, the pentose phosphate pathway and the citric-acid cycle (TCA cycle), which were increased as early as 4 hr post-activation (Figure 2, Panel G). Taken together, these data confirm that strong metabolic changes occur during the first 24 hr post T cell stimulation, prior to cell proliferation.

To investigate potential changes to mitochondrial morphology that accompany these early metabolic changes, first live-cell microscopy was utilized to image mitochondria in T cells isolated from $PhAM^{excised}$ mice, which ubiquitously express a mitochondrial-localized

version of the fluorescent protein dendra-2. Live cell microscopy at 4, 9 and 24 hr post-activation revealed a dramatic increase in mitochondrial mass within 24 hr post T cell stimulation (Figure 2, Panel H). Next mitochondria at 4, 9 and 24 hr post-activation were examined by electron microscopy (EM) (Figure 2, Panel I). Quantification of images demonstrated that single mitochondrial area increased by 2- and 4-fold at 9 and 24 hr post-activation, respectively, when compared to naïve T cells (Figure 2, Panel J). As expected, activation induced cell growth (Figures 1, Panel C), but the relative area of the mitochondria/cytosol increased significantly by 9 hr and 24 hr (Figure 2, Panel K). Mitochondrial number (Figure 2. Panel L) and mitochondrial DNA (mtDNA; Figure 2, Panel M) doubled by 24 hr. Taken together, these studies reveal a unique model of robust and highly synchronized mitochondrial biogenesis during early T cell activation.

Further evidence of synchronicity was apparent from distinct stages of mitochondrial morphology. Naïve $CD4^+$ T cells contained fragmented, rounded mitochondria. After 9 hr, mitochondria appeared hyperfused, and this elongated intermediate resolved back to a fragmented morphology by 24 hr (Figure 2, Panels I and N).

Substantial changes in mitochondrial function also occurred during this early activation period. Even prior to the morphological changes (4 hr post-activation), increased mitochondrial respiration and higher respiratory capacity was measured (Figure 1, Panels D-H). After mitochondria proliferated (24 hr post-activation), basal respiration reached full capacity, which was 10-fold increased compared to resting cells (Figures 2, Panel O and Figure 1, Panel F-G), leaving no spare respiratory capacity (Figure 1P). Cellular ATP as a functional output of respiration was also confirmed. Levels of ATP were initially unchanged, but by 24 hr T cells contained 10-fold higher ATP (Figure 1, Panel H), reflective of increased total purine pools, combined with respiration serving to maintain adenosine nucleotides primarily in the ATP form. Thus, T cells induce a program of synchronized mitochondrial activation and biogenesis, that occurs within 24 hr, and is denoted by increased number of mitochondria which function at their maximal respiratory rate.

Example 2 - Quantitative proteomics identified one-carbon metabolism as the most induced mitochondrial metabolic pathway upon naïve $CD4^+$ T cell activation

To quantitate protein composition, tandem mass spectrometry was used after isobaric peptide tagging to identify proteins that change in concentration during T cell activation (Figure 3, Panel A). Over 5500 proteins and their expression kinetics were quantified during the first 24 hr of T cell activation, which was prior to any cell division (Supplementary List

1). Reproducibility was high between biological replicates (Figure 3, Panel B, and Figure 4, Panel A). By 24 hr post-activation, the majority of cellular proteins were increased by at least 2-fold (Figure 3, Panel C), as anticipated given the massive cell growth (Figure 2, Panel B). Proteins could be grouped into unique clusters according to kinetics and magnitude of induction, with some proteins induced more than 500-fold within 24 hr (Figure 3, Panels D and E, Figure 4, Panel B). Cluster 1 (induced 6-100 fold at 4 hours), represented the earliest-induced proteins, which could be 'drivers' of T cell activation. Consistent with this idea, cluster 1 included well-known early T cell activation markers (CD69 and CD25) and transcriptional regulators of T cell activation and function (MYC, NR4A, JUNB, NFKBID; Figure 3, Panel F). Thus, this dataset may serve as a hypothesis-generating tool for identifying novel immune regulators, as well as more broadly for identifying drivers of exit from quiescence and/or entry into cell cycle.

Intriguingly, 5,10-methenyltetrahydrofolate synthetase (MTHFS), which converts a storage form of folate-bound one-carbon units (5-formyl-THF) into usable one-carbon units (5,10-methylene-THF), was the most-up-regulated metabolic enzyme within the early-induced cluster 1. Unexpectedly, metabolic pathways previously associated with activated T cells, like glycolysis, pentose phosphate pathway, and oxidative phosphorylation were enriched within clusters 5 and 6, which represented the groups of least-induced proteins (Figure 3, Panel E). Instead, the protein clusters associated with high induction were enriched for enzymes of lipid biosynthesis (cluster 2) and nucleotide metabolism (clusters 3 and 4; Figure 3, Panel E). Thus, the proteomic data point to major nodes of metabolic reprogramming yet to be examined in T cell activation.

To examine specifically the mitochondrial proteome upon T cell activation, the MitoCarta database was used as a filter to generate a list of 552 mitochondrial proteins detected. In agreement with the large increase in mitochondrial mass (Figure 2), most mitochondrial proteins were induced upon $CD4^+$ T cell activation (Figure 5, Panel A). Within the mitochondrial proteome, a high degree of variability was observed in the magnitude of induction, ranging from only 2-fold to greater than 200-fold (Figure 5, Panel A), indicating that mitochondrial biogenesis is accompanied by substantial mitochondrial proteome remodeling. To identify the pathways enriched or underrepresented during T cell activation, gene set enrichment analysis was performed on the complete mitochondrial protein list, based on the protein's individual induction Z score at each time point (Figure 5, Panel B). One-carbon metabolism was the only significantly induced pathway, while fatty

acid catabolism, TCA cycle and oxidative phosphorylation were among the suppressed pathways (Figure 5, Panel B).

Next, mitochondrial proteins were classified into four clusters (clusters 1-4), based on the kinetics and magnitude of induction (Figure 5, Panel C). Kegg pathway analysis of each cluster highlighted one-carbon metabolism (folate cycle) as the only significantly enriched pathway in cluster 1 that represents the earliest and most highly induced proteins (Figure 5, Panel C). Interestingly, this analysis also identified significant enrichment in enzymes involved in oxidative phosphorylation, and TCA cycle in the least-induced clusters, whose proteome fraction decreases during T cell activation (3 and 4). This selective elevation of enzymes in the mitochondrial one-carbon pathway compared to the TCA cycle, electron transport chain, and fatty acid oxidation was apparent when compared to the levels of individual proteins within these pathways (Figure 5, Panels D and E). While enzymes of the TCA cycle and electron transport chain were induced similarly to porin induction, enzymes involved in fatty acid β-oxidation were significantly under represented. In contrast, enzymes in the one-carbon metabolic pathway were induced 6-30 fold greater than porin (Figure 5, Panels D and E). Taken together, the analysis of the mitochondrial proteome demonstrated that T cell activation induces mitochondrial proliferation and causes a global change in mitochondrial protein composition with enrichment in enzymes of one-carbon metabolism (Figure 5, Panels D-F).

Example 3 - Enzymes of the one-carbon metabolic pathway are induced in vivo during T cell activation

To validate this unique proteomic signature associated with an increase in enzymes of one-carbon metabolism, a set of antibodies were optimized that could be used to probe the proteins by Western blotting or FACS analysis. First, the expression of enzymes in the one-carbon metabolic pathway in naive $CD4^+$ T cells were compared with $CD4^+$ T cells activated in vitro by Western blotting. A massive induction of enzymes were observed in the one-carbon metabolic pathway (SHMT1, SHMT2, MTHFD1, MTHFD2, MTHFD2L), as well as in enzymes of pyrimidine biosynthesis (DHODH, UMPS), consistent with their increase in the proteomic dataset. This observation contrasted with metabolic proteins that were not significantly elevated (MDH2, OGDH, ASL), or proteins that were significantly under expressed (CPT1A, OTC) in the proteomic dataset (Figures 7, Panels A-B and Figure 6).

To examine if this mitochondrial and metabolic rewiring could be observed upon activation of naïve $CD4^+$ T cells in vivo, expression of metabolic enzymes in T cells after in

vivo activation was temporally examined. To assess antigen-specific T cell responses in vivo, myelin oligodendrocyte (MOG) antigen-specific 2D2 TCR transgenic $CD4^+$ T cells were transferred into C57Bl/6J wild-type mice, the mice were immunized with MOG 35-55 peptide, and antigen-specific T cells isolated from the draining lymph nodes were analyzed by flow cytometry on days 2, 3 and 4 after immunization. (Figure 7, Panel C). As anticipated, 2D2 TCR transgenic T cells (TCR $V\alpha3.2^+/V\beta11^+$) accumulated in the draining lymph nodes (Figure 7, Panel D) and proliferated (Figure 7, Panel E). Consistent with their activation and proliferation, CD69, an early T cell activation marker, was induced only on MOG-specific T cells following immunization (Figure 7, Panel F).

Next, mitochondrial reprograming was assessed in activated MOG-specific $CD4^+$ T cells by measuring the expression of enzymes involved in one-carbon metabolism and pyrimidine biosynthesis by flow cytometry. For these studies, antibodies to enzymes were evaluated that had been validated ex vivo (Figures 7, Panels A-B) and which antibodies could visualize these enzymes by flow cytometry was determined. Strikingly, many of these enzymes were induced in antigen-specific T cells as early as 2 days post immunization (Figure 7, Panel G), in parallel to induction of CD69 (Figure 7, Panel F) and prior to cell division (Figure7, Panel E). Thus, the proteomic dataset was utilized to define a distinct metabolic signature (specified by high levels of cytosolic and mitochondrial enzymes in the one-carbon metabolic and pyrimidine pathway), which can provide a novel tool for probing of the early metabolic activation of T cells in vivo.

Example 4 - T cells activate the mitochondrial arm of one-carbon metabolism

Carbon units derived from the folate-dependent one-carbon pathway are used for thymidylate and de-novo purine biosynthesis. In addition, existing purine derivatives, like hypoxanthine, can be recycled in salvage pathways to generate new purines (Figure 8, Panel A). Thus, initially one-carbon metabolism in T cells was assessed by performing mass spectrometry to examine the levels of these metabolites during T cell activation. Consistent with proteomic data, IMP (inosine monophosphate), generated by purine salvage and de novo biosynthesis, was induced by 4-6 fold as early as 4 hr post-activation (Figure 8, Panel B). Interestingly, by 24 hr, the intracellular level of AICAR, a substrate that precedes IMP in de novo purine biosynthesis was highly induced (10-13 fold), while hypoxanthine, a substrate used for IMP synthesis in the purine salvage pathway was depleted (Figure 8, Panel B). Furthermore, analysis of metabolite content in the growth media highlighted hypoxanthine as the most depleted metabolite by 24 hr post-activation (Figure 8, Panel C).

Together, these results suggest that T cells engage purine salvage and de novo biosynthesis early upon activation.

To test directly whether metabolic flux thru the one-carbon pathway was induced by T cell activation, naïve $CD4^+$ T cells were stimulated in media containing uniformly labeled $^{13}C_3$-serine (U^{13}C-serine). Metabolism of U-^{13}C-labeled serine by the one-carbon metabolic pathway generates uniformly labeled U-$^{13}C_2$-glycine and ^{13}C-labeled 10-formyl-THF, which are consumed by the de novo purine biosynthetic pathway, resulting in ^{13}C labeling of purines (Figure 8, Panel D). The extent of ^{13}C incorporation into the de novo synthesized purines was monitored. Incorporation of one molecule of ^{13}C 10-formyl-THF will give rise to a mass of m+1. m+2 is the result of incorporation of two molecules of ^{13}C 10-formyl-THF or one labeled $^{13}C_2$-glycine. m+3 indicates addition of one molecule of ^{13}C 10-formyl-THF and one labeled $^{13}C_2$-glycine, and m+4 is the result of addition of two ^{13}C 10-formyl-THF molecules and one labeled $^{13}C_2$-glycine. IMP labeling was evident after 4 hr of activation, followed by the labeling of down-stream purine species (ADP and GDP) at 9 hr post-activation (Figure 8, Panel E). Labeling patterns were consistent across many purine species detected by mass spectrometry (Figure 9, Panels A-E).

Mammalian cells contain parallel pathways in the mitochondria and cytosol for generating one-carbon units from serine, and enzymes of both cellular compartments are highly induced with T cell activation (Figures 5 and 7). To test whether both compartments contributed to production of one-carbon units in activated T cells (Figure 8, Panel E), a strategy based on 2,2,3-$^2H_3$-serine (D_3-serine) tracing was utilized (Figure 8, Panel F). Metabolism of D_3-serine via the mitochondrial arm ultimately generates cytosolic methylene-THF (after export from mitochondria as formate) labeled with one deuterium (CDHTHF), whereas direct D_3-serine metabolism by the cytosolic arm generates methylene-THF labeled with two atoms of deuterium (CD_2THF). These two species give rise to dTMP and dTTP labeled with either one or two deuteriums (m+1 and m+2, respectively; Figure 8, Panle F). Analysis of dTMP and dTTP labeling patterns demonstrated a higher fraction of the m+1 compared to m+2 (Figure 8, Panel G). Thus, in activated T cells, the majority of one-carbon units are generated in the mitochondria.

Example 5 - SHMT2 is critical for mitochondrial one-carbon metabolism and T cell survival

Next, the physiological relevance of mitochondrial one-carbon metabolism was probed by studying the effect of the knockdown (KD) of SHMT2, the first enzyme in the mitochondrial arm of one-carbon metabolism (Figure 10, Panel A). In order to genetically

manipulate primary $CD4^+$ T cells and test the effect of loss of SHMT2 on early $CD4^+$ T cell activation, a protocol was developed in which naïve $CD4^+$ T cells were activated with anti-CD3/anti-CD28, transduced 24 hours later with a retroviral vector, rested in IL-2/IL-7 and subsequently restimulated by anti-CD3/anti-CD28 (Figure 11). The 'resting' T cells responded similarly to naïve cells upon re-activation (Figure 2, Panel B-D); reactivation of the 'resting T cells' induced cell growth, up-regulation of the early activation markers CD69, and CD25, and down regulation of CD62L (Figure 11). In addition, reactivation of the resting T cells induced proliferation (Figure 11, Panel C), similar to activation of naïve T cells (Figure 2, Panel D). Reactivation also induced a 2-fold increase in mitochondrial DNA content (Figure 11, Panel D), which was similar in the increase in mitochondrial/nuclear DNA ratio in activated naïve T cell (Figure 2, Panel M). Importantly, this induction of mitochondrial mass was accompanied by a significant increase in SHMT2 expression (Figure 11, Panel E). In sum, restimulated $CD4^+$ T cells showed similar immune activation markers, cell proliferation and mitochondrial biogenesis as naïve T cells.

Using this optimized strategy, naïve $CD4^+$ T cells were infected retrovirus targeting multiple sequences for either GFP^+ sh-LacZ (control sh-1-2) or GFP^+ sh-SHMT2 (SHMT2 sh1-3). After 5 days of 'resting', the cells were sorted for GFP^+ cells, reactivated, and SHMT2 deletion was validated by western blotting (Figure 10, Panel B). Sequences for SHMT2 sh-1 and SHMT2 sh-3 demonstrated efficient knockdown and were used for further experiments. To test whether reduction of SHMT2 blocked mitochondrial one-carbon metabolism, metabolic flux analysis was performed with D_3-serine in the SHMT2 KD and control cells (as in Figure 8, Panel F). These experiments demonstrated that knockdown of SHMT2 decreased the mitochondrial contribution of one-carbon units to the total cellular pool, while increasing the share of one-carbon units derived from the cytosolic pathway (%(m+1) < %(m+2); Figure 10, Panel C).

To examine the impact of inhibiting mitochondrial one-carbon metabolism on de novo purine biosynthesis, LC-MS was used to measure levels of intermediates in the pathway (Figure 10, Panel D). Compared with control cells, SHMT2 knockdown resulted in a massive accumulation of GAR, SAICAR, and AICAR, metabolites upstream of 10-formyl THF incorporation. Notably FGAR, a product of 10-formyl-THF reaction with GAR transformylase, was reduced in SHMT2 sh3 cells, which had the lowest levels of SHMT2 (Figure 10, Panel D). Levels of IMP, which is also downstream of the salvage pathway (Figure 8, Panel A), were not affected (Figure 10, Panel D). These data suggest that the

mitochondrial pathway is critical for supplying one-carbon units for de novo purine synthesis.

Next whether mitochondrial one-carbon metabolism was critical for T cell activation was examined. Early activation markers CD69 and CD25 were measured, and found that levels of these surface molecules were comparable in control and SHMT2 KD T cells (Figure 10, Panel E), indicating that expression of these immune activation markers were not dependent on mitochondrial one-carbon metabolism. Likewise, SHMT2 KD cells displayed comparable cell proliferation to control cells (Figures 10, Panel F and 11, Panel F, respectively), indicating sufficiency of the cytosolic SHMT1 pathway to support initial proliferation. However, T cells with low SHMT2 demonstrated a 2-3-fold increase in cell death compared with control cells, at 48 and 72 hr post-reactivation (Figure 10, Panels G and H and Figure 11, Panels G and H, respectively), demonstrating that the mitochondrial arm of one-carbon metabolism contributes to T cell survival.

To probe the physiological significance of SHMT2 on T cells in vivo, Mog-specific 2D2 $CD4^+$ T cells that had been infected with either GFP^+ SHMT2 sh-3 or GFP^+ control sh-1 vector were adoptively transferred into wild-type recipient mice. The recipient mice were immunized with MOG35-55 peptide in CFA, and assessed GFP^+, antigen-specific T cells in the draining lymph nodes at day 5 post-immunization (Figure 10, Panel I). There were significantly less GFP^+ SHMT2 KD T cells, in the draining lymph nodes compared GFP^+ sh-control T cells (Figure 10, Panel J), and these SHMT2 KD T cells had significantly lower expression of Ki67 compared to GFP^+ sh-control T cells (Figure 10, Panel K). Thus, although one-carbon pathway is an early metabolic indicator, the effects of SHMT2 KD are long lasting in vivo. Taken together, these studies demonstrate that mitochondrial one-carbon metabolism is essential for T cell activation and survival and cannot be fully compensated by increased purine scavenging or flux through cytosolic one-carbon pathway.

Example 6 - A combination of n-acetyl cysteine (NAC) and nicotinamide mononucleotide (NMN) rescues cell death of SHMT2 KD T cells

Resting $CD4^+$ T cells infected with either sh-LacZ (control, sh-1) or sh-SHMT2 (sh-3) were re-activated in media containing different combinations of: formate, NAC and NMN (Figure 12). Treatment with NAC and NMN significantly reduced cell death, suggesting that cell death in SHMT2 KD T cells was driven, at least in part, by oxidative stress and bioenergetics deficiency.

Incorporation by Reference

All publications, patents, and patent applications mentioned herein are hereby incorporated by reference in their entirety as if each individual publication, patent or patent application was specifically and individually indicated to be incorporated by reference. In case of conflict, the present application, including any definitions herein, will control.

Equivalents

Those skilled in the art will recognize, or be able to ascertain using no more than routine experimentation, many equivalents to the specific embodiments described herein. Such equivalents are intended to be encompassed by the following claims.

What is claimed is:

1. A method of treating or preventing an autoimmune disease, an inflammatory disease, a graft-versus host disease or organ transplant rejection in a subject comprising administering to the subject an agent that inhibits the one-carbon metabolic pathway.

2. The method of claim 1, wherein the agent inhibits the activity or expression of SHMT1, SHMT2, MTHFD1, MTHFD2, MTHFD1L or MTHFD2L.

3. The method of claim 1 or claim 2, wherein the agent is a small molecule.

4. The method of claim 3, wherein the small molecule inhibits the activity of SHMT1, SHMT2, MTHFD1, MTHFD2, MTHFD1L or MTHFD2L.

5. The method of claim 1 or claim 2, wherein the agent is an inhibitory polynucleotide.

6. The method of claim 4, wherein the inhibitory polynucleotide is selected from the group consisting of siRNA, shRNA, and an antisense RNA molecule, or is a polynucleotide that encodes a molecule selected from the group consisting of siRNA, shRNA, and an antisense RNA molecule.

7. The method of claim 5 or claim 6, wherein the inhibitory polynucleotide targets SHMT1 mRNA, SHMT2 mRNA, MTHFD1 mRNA, MTHFD2 mRNA, MTHFD1L mRNA or MTHFD2L mRNA.

8. The method of any one of claims 1 to 7, wherein the autoimmune disease, inflammatory disease, graft-versus host disease or organ transplant rejection is an autoimmune disease.

9. The method of claim 8, wherein the autoimmune disease is selected from the group consisting of glomerular nephritis, arthritis, dilated cardiomyopathy-like disease, ulceous colitis, Sjogren syndrome, Crohn's disease, systemic erythematodes, chronic rheumatoid arthritis, multiple sclerosis, psoriasis, allergic contact dermatitis, polymyosiis, pachyderma, periarteritis nodosa, rheumatic fever, vitiligo vulgaris, insulin dependent diabetes mellitus, Behcet disease, Hashimoto disease, Addison disease, dermatomyositis, myasthenia gravis, Reiter syndrome, Graves' disease, anaemia perniciosa, Goodpasture syndrome, sterility disease, chronic active hepatitis, pemphigus, autoimmune thrombopenic purpura, and autoimmune hemolytic anemia, active chronic hepatitis, Addison's disease, anti-phospholipid syndrome, atopic allergy, autoimmune atrophic gastritis, achlorhydra autoimmune, celiac disease, Cushing's syndrome, dermatomyositis, discoid lupus, erythematosis, Hashimoto's thyroiditis, idiopathic adrenal atrophy, idiopathic thrombocytopenia, insulin-dependent diabetes, Lambert-Eaton syndrome, lupoid hepatitis, some cases of lymphopenia, mixed

connective tissue disease, pemphigoid, pemphigus vulgaris, pernicious anema, phacogenic uveitis, polyarteritis nodosa, polyglandular autosyndromes, primary biliary cirrhosis, primary sclerosing cholangitis, Raynaud's syndrome, relapsing polychondritis, Schmidt's syndrome, limited scleroderma (or crest syndrome), sympathetic ophthalmia, systemic lupus erythematosis, Takayasu's arteritis, temporal arteritis, thyrotoxicosis, type b insulin resistance, ulcerative colitis and Wegener's granulomatosis.

10. The method of any one of claims 1 to 7, wherein the autoimmune disease, inflammatory disease, graft-versus host disease or organ transplant rejection is an inflammatory disease.

11. The method of claim 10, wherein the inflammatory disease is selected from the group consisting of inflammatory bowel disease, rheumatoid arthritis, psoriatic arthritis, psoriasis, diabetes mellitus, Alzheimer's disease, refractory asthma, multiple sclerosis, atherosclerosis, and vasculitis.

12. The method of claim 11, wherein the inflammatory disease is an inflammatory bowel disease.

13. The method of claim 12, wherein the inflammatory bowel disease is selected from the group consisting of Crohn's disease, ulcerative colitis, irritable bowel syndrome, microscopic colitis, lymphocytic-plasmocytic enteritis, coeliac disease, collagenous colitis, lymphocytic colitis and eosinophilic enterocolitis.

14. The method of any one of claims 1 to 7, wherein the autoimmune disease, inflammatory disease, graft-versus host disease or organ transplant rejection is graft-versus-host disease.

15. The method of any one of claims 1 to 7, wherein the autoimmune disease, inflammatory disease, graft-versus host disease or organ transplant rejection is organ transplant rejection.

16. The method of any one of claims 1 to 12, wherein the agent inhibits the one-carbon metabolic pathway in T cells of the subject.

17. The method of claim 13, wherein the inhibition of the one-carbon metabolic pathway in the T cells of the subject reduces T cell survival in the subject.

18. The method of any one of claims 1 to 17, wherein the agent is administered intravenously, intramuscularly, intraperitoneally, subcutaneously or orally.

19. A method of treating or preventing a disease or disorder associated with impairment of the one-carbon metabolic pathway in a subject comprising administering to the subject an

agent that increases the activity or expression of SHMT1, SHMT2, MTHFD1, MTHFD2, MTHFD1L or MTHFD2L in the subject.

20. The method of claim 19, wherein the agent is a small molecule.

21. The method of claim 20, wherein the small molecule increases the activity of SHMT1, SHMT2, MTHFD1, MTHFD2, MTHFD1L or MTHFD2L.

22. The method of claim 19, wherein the agent is a polynucleotide.

23. The method of claim 22, wherein the polynucleotide encodes SHMT1, SHMT2, MTHFD1, MTHFD2, MTHFD1L or MTHFD2L.

24. The method of claim 22 or claim 23, wherein the polynucleotide is in a vector.

25. The method of claim 24, wherein the vector is a viral vector, a retroviral vector, a bacterial vector or a plasmid vector.

26. The method of claim 22 or claim 23, wherein the polynucleotide is a mRNA.

27. The method of any one of claims 19 to 26, wherein the subject has an impaired immune system.

28. The method of claim 27, wherein the subject has reduced numbers of activated T cells.

29. The method of any one of claims 19 to 28, wherein the subject has a disease or disorder selected from the group consisting of Smith-Magenis Syndrome (SHMT1 deletion), MTHFR deficiency, MTHFD1 deficiency, schizophrenia (MTHFR polymorphism), depression (methionine sulfoxide reductase), AD-MTHFR and MTR polymorphism, cobalamine deficiency and rranscobalamine deficiency.

30. The method of any one of claims 19 to 29, wherein the agent increases the activity or expression of SHMT1, SHMT2, MTHFD1, MTHFD2, MTHFD1L or MTHFD2L in T cells of the subject.

31. The method of claim 30, wherein the inhibition of SHMT1, SHMT2, MTHFD1, MTHFD2, MTHFD1L or MTHFD2L in the T cells of the subject increases T cell survival in the subject.

32. The method of any one of claims 19 to 31, wherein the agent is administered intravenously, intramuscularly, intraperitoneally, subcutaneously or orally.

33. A method of detecting T cell activation comprising detecting the level of SHMT1, SHMT2, MTHFD1, MTHFD2, MTHFD1L or MTHFD2L in a T cell.

34. The method of claim 33, wherein the level of SHMT1, SHMT2, MTHFD1, MTHFD2, MTHFD1L or MTHFD2L is detected using an antibody that specifically binds to SHMT1, SHMT2, MTHFD1, MTHFD2, MTHFD1L or MTHFD2L.

35. The method of claim 34, wherein the antibody is detectably labeled.

36. The method of claim 35, wherein the detectable label is a fluorescent label.

37. The method of any one of claims 33 to 36, wherein the level of SHMT1, SHMT2, MTHFD1, MTHFD2, MTHFD1L or MTHFD2L is detected by flow cytometry or fluorescent microscopy.

38. The method of any one of claims 33 to 37, wherein the T cell is in a tissue sample.

39. The method of claim 38, wherein the tissue sample is a tumor biopsy sample, or a lymph node biopsy sample.

40. The method of any one of claim 33 to 37, wherein the T cell is from a blood sample.

41. A method of detecting an autoimmune disease, an inflammatory disease, a graft-versus host disease or organ transplant rejection in a subject comprising detecting the level of SHMT1, SHMT2, MTHFD1, MTHFD2, MTHFD1L or MTHFD2L expressed by T cells in the subject.

42. The method of claim 41, wherein the autoimmune disease, inflammatory disease, graft-versus host disease or organ transplant rejection is an autoimmune disease.

43. The method of claim 42, wherein the autoimmune disease is selected from the group consisting of glomerular nephritis, arthritis, dilated cardiomyopathy-like disease, ulceous colitis, Sjogren syndrome, Crohn's disease, systemic erythematodes, chronic rheumatoid arthritis, multiple sclerosis, psoriasis, allergic contact dermatitis, polymyosiis, pachyderma, periarteritis nodosa, rheumatic fever, vitiligo vulgaris, insulin dependent diabetes mellitus, Behcet disease, Hashimoto disease, Addison disease, dermatomyositis, myasthenia gravis, Reiter syndrome, Graves' disease, anaemia perniciosa, Goodpasture syndrome, sterility disease, chronic active hepatitis, pemphigus, autoimmune thrombopenic purpura, and autoimmune hemolytic anemia, active chronic hepatitis, Addison's disease, anti-phospholipid syndrome, atopic allergy, autoimmune atrophic gastritis, achlorhydra autoimmune, celiac disease, Cushing's syndrome, dermatomyositis, discoid lupus, erythematosis, Hashimoto's thyroiditis, idiopathic adrenal atrophy, idiopathic thrombocytopenia, insulin-dependent diabetes, Lambert-Eaton syndrome, lupoid hepatitis, some cases of lymphopenia, mixed connective tissue disease, pemphigoid, pemphigus vulgaris, pernicious anema, phacogenic uveitis, polyarteritis nodosa, polyglandular autosyndromes, primary biliary cirrhosis, primary

sclerosing cholangitis, Raynaud's syndrome, relapsing polychondritis, Schmidt's syndrome, limited scleroderma (or crest syndrome), sympathetic ophthalmia, systemic lupus erythematosis, Takayasu's arteritis, temporal arteritis, thyrotoxicosis, type b insulin resistance, ulcerative colitis and Wegener's granulomatosis.

44. The method of claim 41, wherein the autoimmune disease, inflammatory disease, graft-versus host disease or organ transplant rejection is an inflammatory disease.

45. The method of claim 44, wherein the inflammatory disease is selected from the group consisting of inflammatory bowel disease, rheumatoid arthritis, psoriatic arthritis, psoriasis, diabetes mellitus, Alzheimer's disease, refractory asthma, multiple sclerosis, atherosclerosis, and vasculitis.

46. The method of claim 45, wherein the inflammatory disease is an inflammatory bowel disease.

47. The method of claim 46, wherein the inflammatory bowel disease is selected from the group consisting of Crohn's disease, ulcerative colitis, irritable bowel syndrome, microscopic colitis, lymphocytic-plasmocytic enteritis, coeliac disease, collagenous colitis, lymphocytic colitis and eosinophilic enterocolitis.

48. The method of claim 41, wherein the autoimmune disease, inflammatory disease, graft-versus host disease or organ transplant rejection is graft-versus-host disease.

49. The method of claim 41, wherein the autoimmune disease, inflammatory disease, graft-versus host disease or organ transplant rejection is organ transplant rejection.

50. The method of any one of claims 41 to 49, wherein the level of SHMT1, SHMT2, MTHFD1, MTHFD2, MTHFD1L or MTHFD2L is detected using an antibody that specifically binds to SHMT1, SHMT2, MTHFD1, MTHFD2, MTHFD1L or MTHFD2L.

51. The method of claim 50, wherein the antibody is detectably labeled.

52. The method of claim 51, wherein the detectable label is a fluorescent label.

53. The method of any one of claims 41 to 52, wherein the level of SHMT1, SHMT2, MTHFD1, MTHFD2, MTHFD1L or MTHFD2L is detected by flow cytometry or fluorescent microscopy.

54. The method of any one of claims 41 to 53, wherein the T cells are in a tissue sample.

55. The method of claim 54, wherein the tissue sample is a tumor biopsy sample, or a lymph node biopsy sample.

56. The method of any one of claim 41 to 53, wherein the T cells are from a blood sample.

57. A method of determining the efficacy of an immunotherapy in a subject comprising detecting the level of SHMT1, SHMT2, MTHFD1, MTHFD2, MTHFD1L or MTHFD2L expressed by T cells in the subject.

58. The method of claim 57, wherein the immunotherapy is a vaccine.

59. The method of claim 57, wherein the subject has cancer.

60. The method of claim 59, wherein the immunotherapy comprises administering an immune checkpoint inhibitor to the subject.

61. The method of claim 60, wherein the immune checkpoint inhibitor is an antibody or antigen-binding fragment thereof that specifically binds to an immune checkpoint protein.

62. The method of claim 61, wherein the immune checkpoint protein is selected from the group consisting of CTLA4, PD-1, PD-L1, PD-L2, A2AR, B7-H3, B7-H4, BTLA, KIR, LAG3, TIM-3 or VISTA.

63. The method of claim 60, wherein the immune checkpoint inhibitor is selected from the group consisting of nivolumab, pembrolizumab, pidilizumab, AMP-224, AMP-514, STI-A1110, TSR-042, RG-7446, BMS-936559, MEDI-4736, MSB-0020718C, AUR-012 and STI-A1010.

64. The method of claim 59, wherein the immunotherapy comprises administering a cancer vaccine to the subject.

65. The method of claim 59, wherein the immunotherapy comprises administering a cancer-specific T cell to the subject.

66. The method of claim 65, wherein the cancer-specific T cell expresses a chimeric antigen receptor.

67. The method of any one of claims 57 to 66, wherein the immunotherapy comprises administering an adjuvant to the subject.

68. The method of claim 67, wherein the adjuvant is selected from the group consisting of an immune modulatory protein, Adjuvant 65, α-GalCer, aluminum phosphate, aluminum hydroxide, calcium phosphate, β-Glucan Peptide, CpG DNA, GPI-0100, lipid A, lipopolysaccharide, Lipovant, Montanide, N-acetyl-muramyl-L-alanyl-D-isoglutamine, Pam3CSK4, quil A and trehalose dimycolate.

69. The method of any one of claims 57 to 68, wherein the level of SHMT1, SHMT2, MTHFD1, MTHFD2, MTHFD1L or MTHFD2L is detected using an antibody that specifically binds to SHMT1, SHMT2, MTHFD1, MTHFD2, MTHFD1L or MTHFD2L.

70. The method of claim 69, wherein the antibody is detectably labeled.

71. The method of claim 70, wherein the detectable label is a fluorescent label.

72. The method of any one of claims 57 to 71, wherein the level of SHMT1, SHMT2, MTHFD1, MTHFD2, MTHFD1L or MTHFD2L is detected by flow cytometry or fluorescent microscopy.

73. The method of any one of claims 57 to 72, wherein the T cells are in a tissue sample.

74. The method of claim 73, wherein the tissue sample is a tumor biopsy sample, or a lymph node biopsy sample.

75. The method of any one of claim 57 to 72, wherein the T cells are from a blood sample.

76. A method of detecting T cell exhaustion in a subject comprising detecting the level of SHMT1, SHMT2, MTHFD1, MTHFD2, MTHFD1L or MTHFD2L expressed by T cells in the subject.

77. The method of claim 76, wherein the subject is elderly.

78. The method of claim 76 or 77, wherein the level of T cell exhaustion is being detected to determine whether the subject is a suitable candidate for an immunotherapy.

79. The method of claim 78, wherein the immunotherapy is a vaccine.

80. The method of any one of claims 76 to 79, wherein the level of SHMT1, SHMT2, MTHFD1, MTHFD2, MTHFD1L or MTHFD2L is detected using an antibody that specifically binds to SHMT1, SHMT2, MTHFD1, MTHFD2, MTHFD1L or MTHFD2L.

81. The method of claim 80, wherein the antibody is detectably labeled.

82. The method of claim 81, wherein the detectable label is a fluorescent label.

83. The method of any one of claims 76 to 82, wherein the level of SHMT1, SHMT2, MTHFD1, MTHFD2, MTHFD1L or MTHFD2L is detected by flow cytometry or fluorescent microscopy.

84. The method of any one of claims 76 to 83, wherein the T cells are in a tissue sample.

85. The method of claim 84, wherein the tissue sample is a tumor biopsy sample, or a lymph node biopsy sample.

86. The method of any one of claim 76 to 83, wherein the T cells are from a blood sample.

87. The method of any one of claims 1 to 32 and 41 to 86, wherein the subject is a human subject.

88. A method of treating or preventing a cancer in a subject comprising administering to the subject an agent that increases the activity or expression of SHMT2 in the subject.

89. The method of claim 88, wherein the cancer is associated with impairment of the one-carbon metabolic pathway.

90. The method of claim 88 or 89, wherein the agent is a small molecule.

91. The method of claim 90, wherein the small molecule increases the activity of SHMT2.

92. The method of claim 88 or 89, wherein the agent is a polynucleotide.

93. The method of claim 92, wherein the polynucleotide encodes SHMT2.

94. The method of claim 92, wherein the polynucleotide is in a vector.

95. The method of claim 94, wherein the vector is a viral vector, a retroviral vector, a bacterial vector or a plasmid vector.

96. The method of claim 92 or claim 93, wherein the polynucleotide is a mRNA.

97. The method of any one of claims 88 to 96, wherein the agent is administered intravenously, intramuscularly, orally, or locally.

98. The method of any one of claims 88 to 96, wherein the agent is administered with an additional agent.

99. The method of claim 98, wherein the additional agent is a chemotherapeutic agent.

100. The method of claim 98, wherein the additional agent is an immune checkpoint inhibitor.

101. A method of increasing tumor infiltrating T cell activity or function in a subject comprising administering to the subject an agent that increases the activity or expression of SHMT2 in the subject.

102. A method of treating a tumor in a subject comprising administering to the subject an agent that increases the activity or expression of SHMT2 in the subject.

103. The method of claim 102, wherein the tumor is an adenocarcinoma, an adrenal tumor, an anal tumor, a bile duct tumor, a bladder tumor, a bone tumor, a brain/CNS tumor, a breast tumor, a cervical tumor, a colorectal tumor, an endometrial tumor, an esophageal tumor, an Ewing tumor, an eye tumor, a gallbladder tumor, a gastrointestinal, a kidney tumor, a laryngeal or hypopharyngreal tumor, a liver tumor, a lung tumor, a mesothelioma tumor, a multiple myeloma tumor, a muscle tumor, a nasopharyngeal tumor, a nueroblastoma, an oral tumor, an osteosarcoma, an ovarian tumor, a pancreatic tumor, a penile tumor, a pituitary tumor, a primary tumor, a prostate tumor, a retinoblastoma, a Rhabdomyosarcoma, a salivary gland tumor, a soft tissue sarcoma, a melanoma, a metastatic tumor, a basal cell carcinoma, a

Merkel cell tumor, a testicular tumor, a thymus tumor, a thyroid tumor, a uterine tumor, a vaginal tumor, a vulvar tumor, or a Wilms tumor.

104. The method of any one of claims 101 to 103, wherein the agent is a small molecule.

105. The method of claim 104, wherein the small molecule increases the activity of SHMT2.

106. The method of any one of claims 101 to 103, wherein the agent is a polynucleotide.

107. The method of claim 106, wherein the polynucleotide encodes SHMT2.

108. The method of claim 106, wherein the polynucleotide is in a vector.

109. The method of claim 108, wherein the vector is a viral vector, a retroviral vector, a bacterial vector or a plasmid vector.

110. The method of claim 106 or claim 107, wherein the polynucleotide is a mRNA.

111. The method of any one of claims 101 to 110, wherein the agent is administered intravenously, intramuscularly, orally, or locally.

112. The method of any one of claims 101 to 111, wherein the agent is administered with an additional agent.

113. The method of claim 112, wherein the additional agent is a chemotherapeutic agent.

114. The method of claim 112, wherein the additional agent is an immune checkpoint inhibitor.

115. The method of any one of claims 101 to 114, wherein the subject has cancer.

116. A method of reducing age-related T cell dysfunction in a subject comprising administering to the subject an agent that activates one-carbon metabolic pathway.

117. The method of claim 116, wherein the agent increases the activity or expression of SHMT2 in the subject.

118. A method of increasing T cell growth comprising administering to the subject an agent that increases the activity or expression of SHMT2 in the subject.

119. The method of claim 118, wherein the agent is formate.

Figure 1

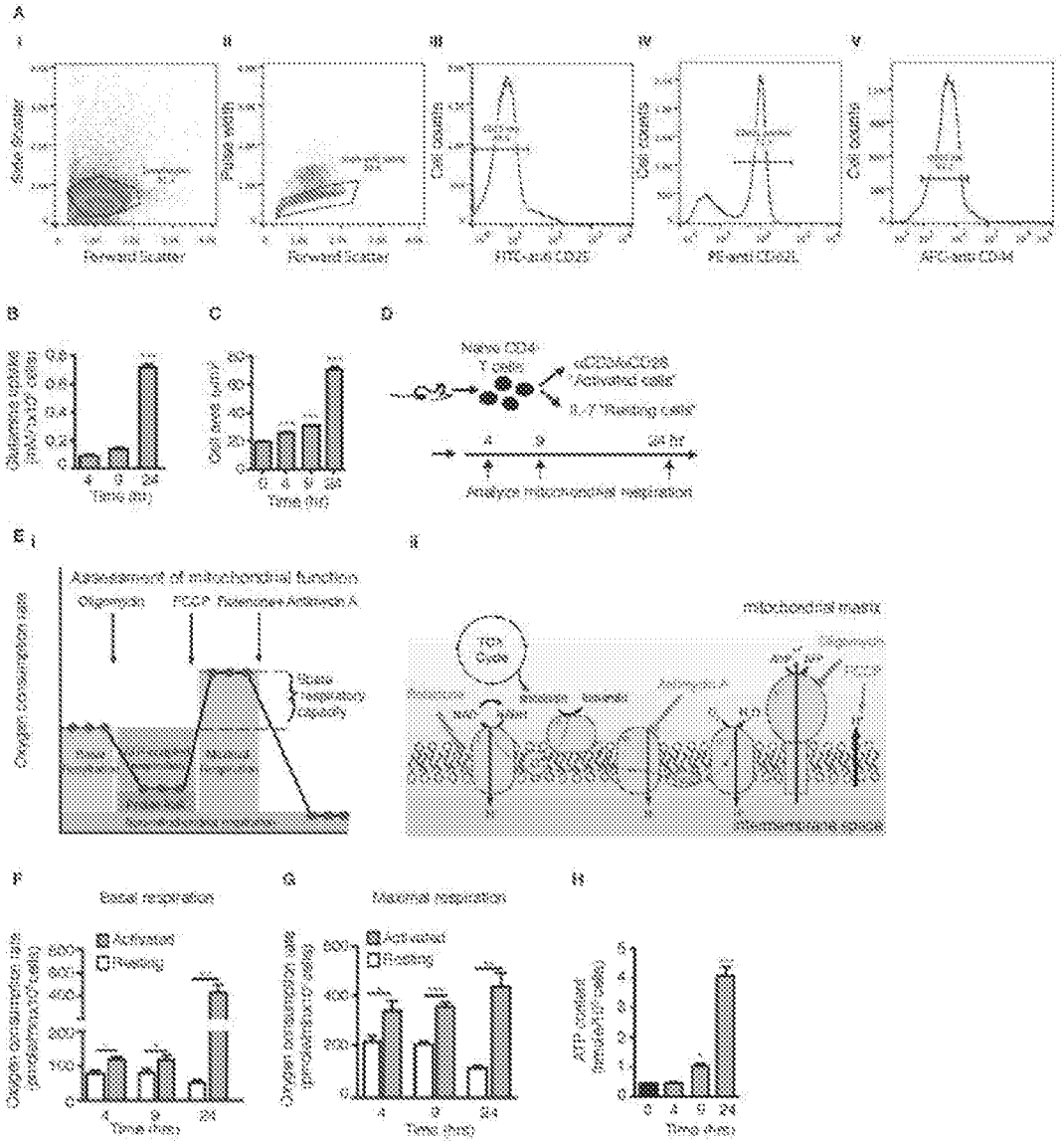

A
Forward Scatter
Forward Scatter
Time (hr)
Time (hr)
Naive CD4+ T cells
αCD3/αCD28 Activated cells
IL-7 "Resting cells"
Analyze mitochondrial respiration
Assessment of mitochondrial function
Oligomycin
FCCP
Rotenone/Antimycin A
Basal respiration
Maximal respiration
Activated
Resting
Time (hrs)
Time (hrs)
Time (hrs)

Figure 2

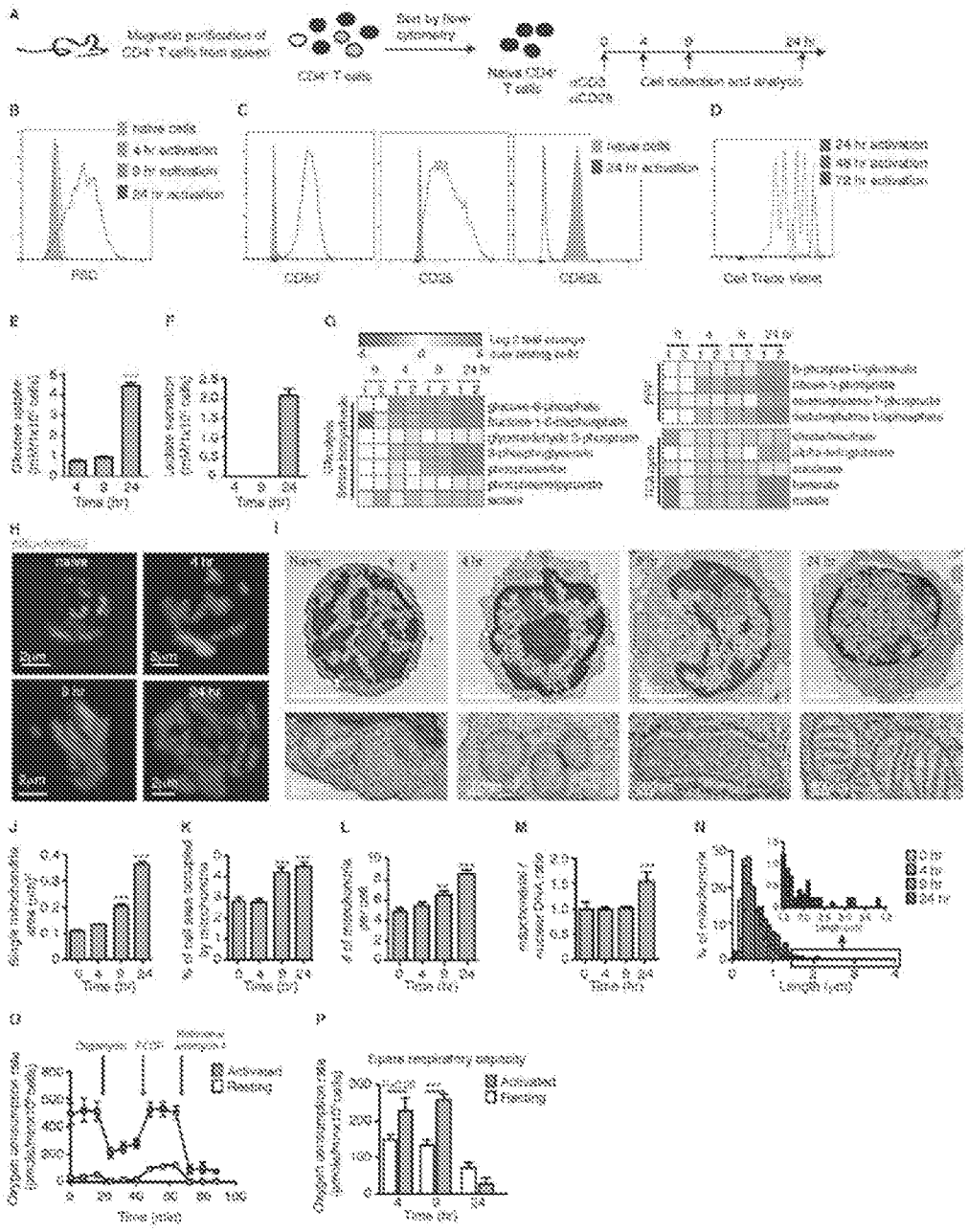
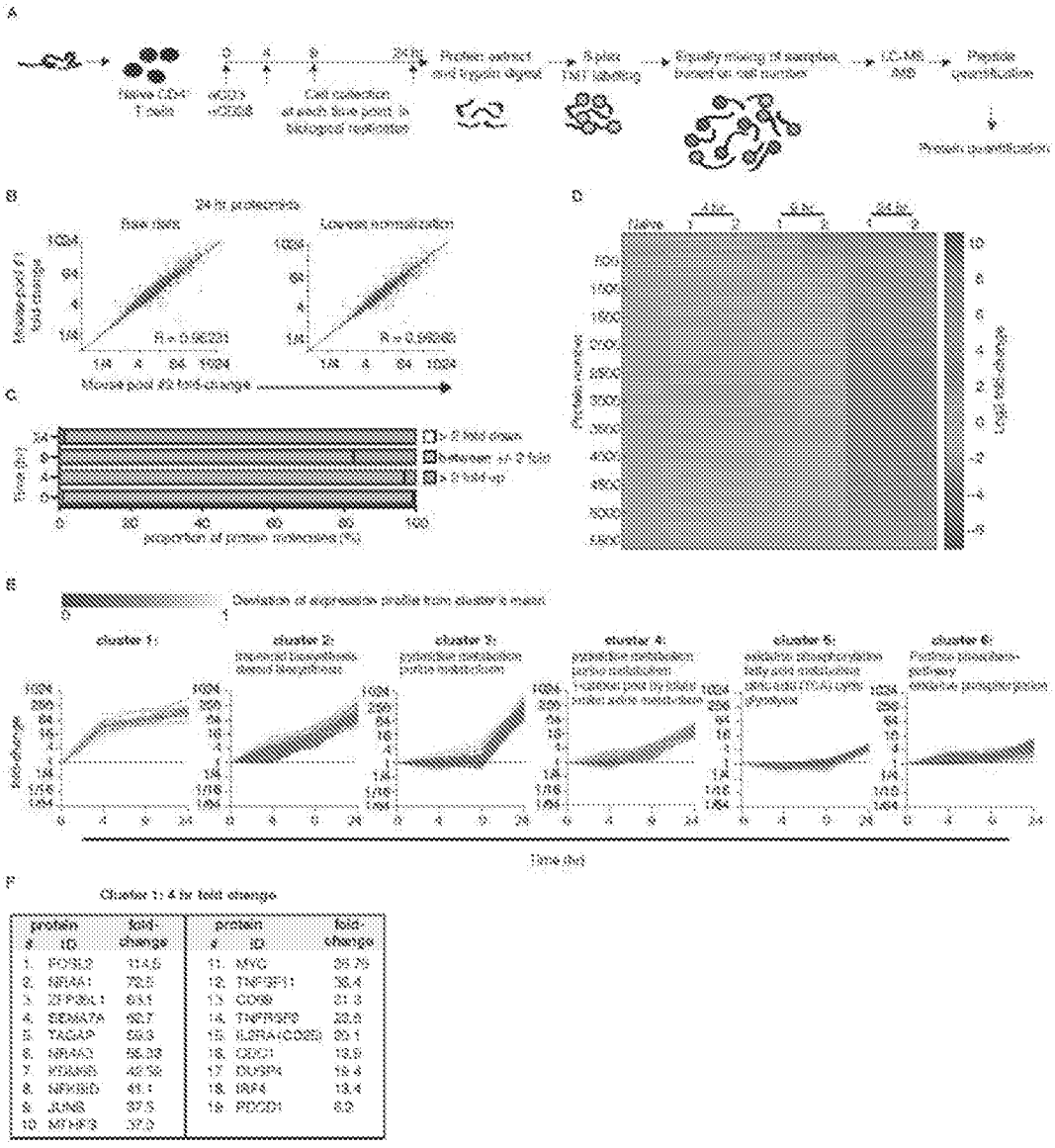


Figure 3



F

Cluster 1: 4 hr fold change

protein #	protein ID	fold change	protein #	protein ID	fold change
1	PCSK9	114.6	11	MYC	66.75
2	SERAA1	76.0	12	TNFSF11	36.4
3	ZFP36L1	63.1	13	CCR8	31.6
4	SEMA7A	60.7	14	TNFRSF8	22.6
5	TAGAP	56.3	15	IL2RA (CD25)	20.1
6	NR4A3	46.28	16	CD01	19.9
7	PTAMS	46.16	17	DUSP4	19.4
8	NFKBID	41.1	18	IRF4	13.4
9	JUNB	37.5	19	PDCD1	8.9
10	MTHFD	37.0			

Figure 4

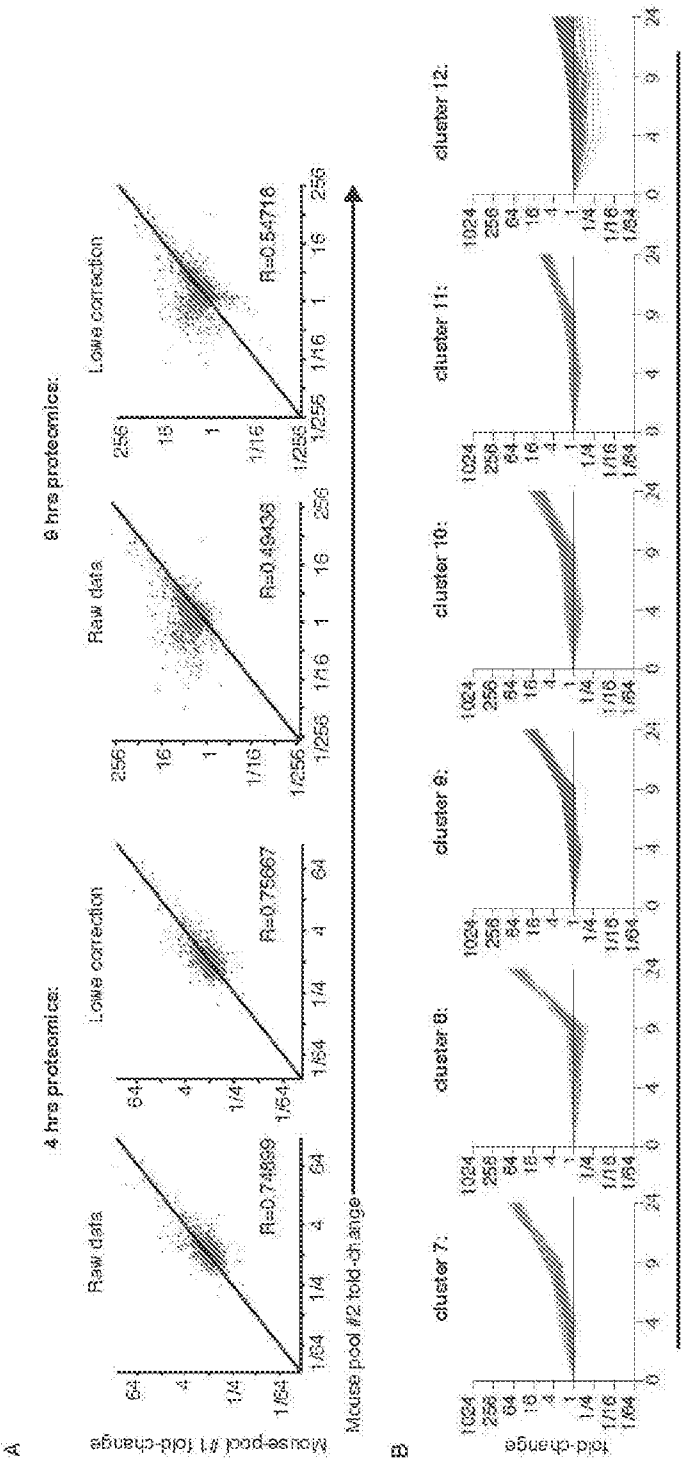

A
4 hrs proteomics:
8 hrs proteomics:
Raw data
Lowe correction
Raw data
Lowe correction
R=0.748639
R=0.755667
R=0.493436
R=0.547716
Mouse pool #1 fold-change
Mouse pool #2 fold-change
B
cluster 7:
cluster 8:
cluster 9:
cluster 10:
cluster 11:
cluster 12:
fold-change
Time (hrs)

Figure 5

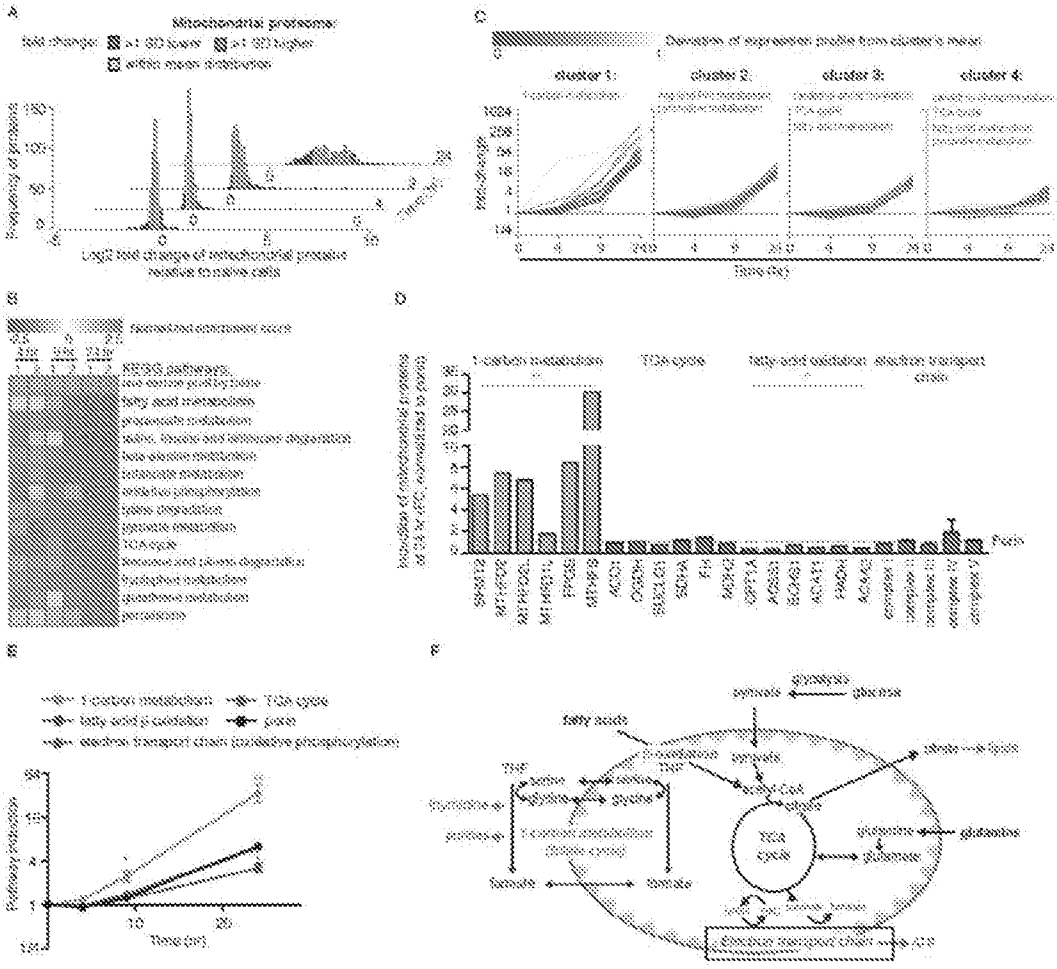

A
Mitochondrial proteome
fold change:
within mean distribution
Log2 fold change of mitochondrial proteins relative to naive cells
C
Deviation of expression profile from cluster's mean
cluster 1:
cluster 2:
cluster 3:
cluster 4:
Time (hr)
B
RENG pathways:
fatty acid metabolism
propanoate metabolism
valine, leucine and isoleucine degradation
TCA cycle
pyruvate metabolism
oxidative phosphorylation
peroxisome
D
1 carbon metabolism
TCA cycle
fatty acid oxidation
electron transport chain
Fold change of mitochondrial proteins at 72 hr PCI, normalized to naive
Pvalue
E
1 carbon metabolism
TCA cycle
fatty acid β oxidation
purine
electron transport chain (oxidative phosphorylation)
Pathway activation
Time (hr)
F
glycolysis
pyruvate
glucose
fatty acids
TCA cycle
glutamine
glutathione
electron transport chain
ATP

Figure 6

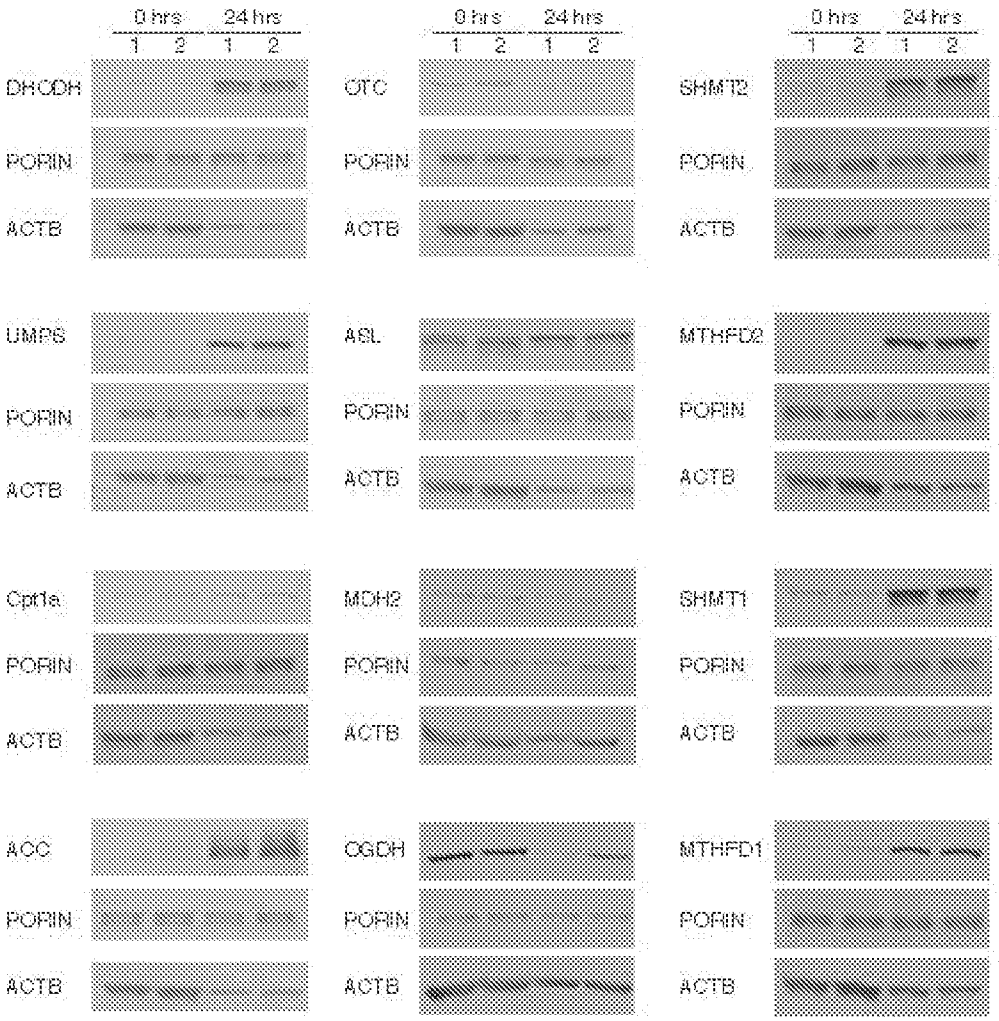

0 hrs
24 hrs
1 2 1 2
DHODH
PORIN
ACTB
OTC
PORIN
ACTB
SHMT2
PORIN
ACTB
UMPS
PORIN
ACTB
ASL
PORIN
ACTB
MTHFD2
PORIN
ACTB
Cpt1a
PORIN
ACTB
MDH2
PORIN
ACTB
SHMT1
PORIN
ACTB
ACC
PORIN
ACTB
OGDH
PORIN
ACTB
MTHFD1
PORIN
ACTB

Figure 7

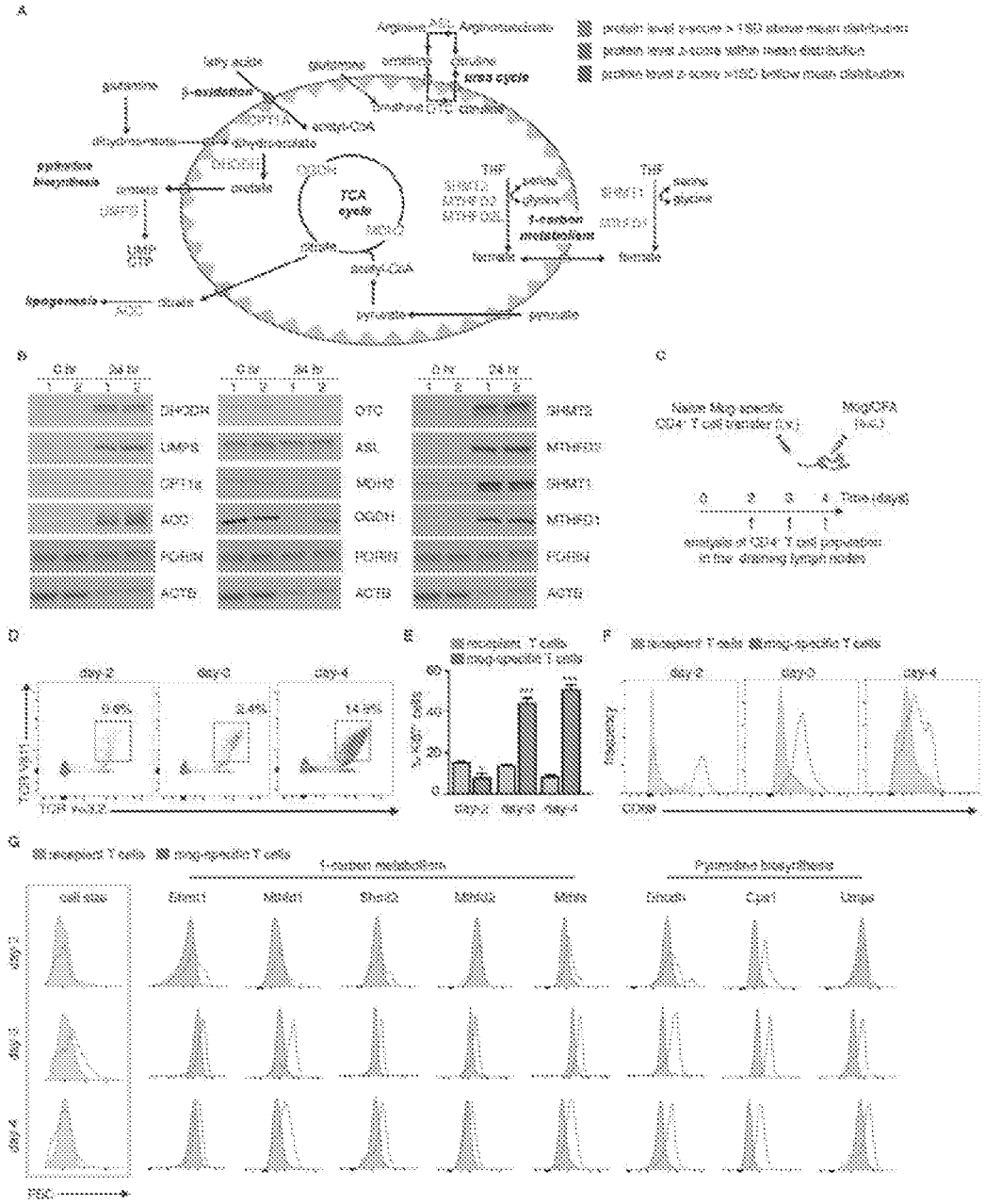
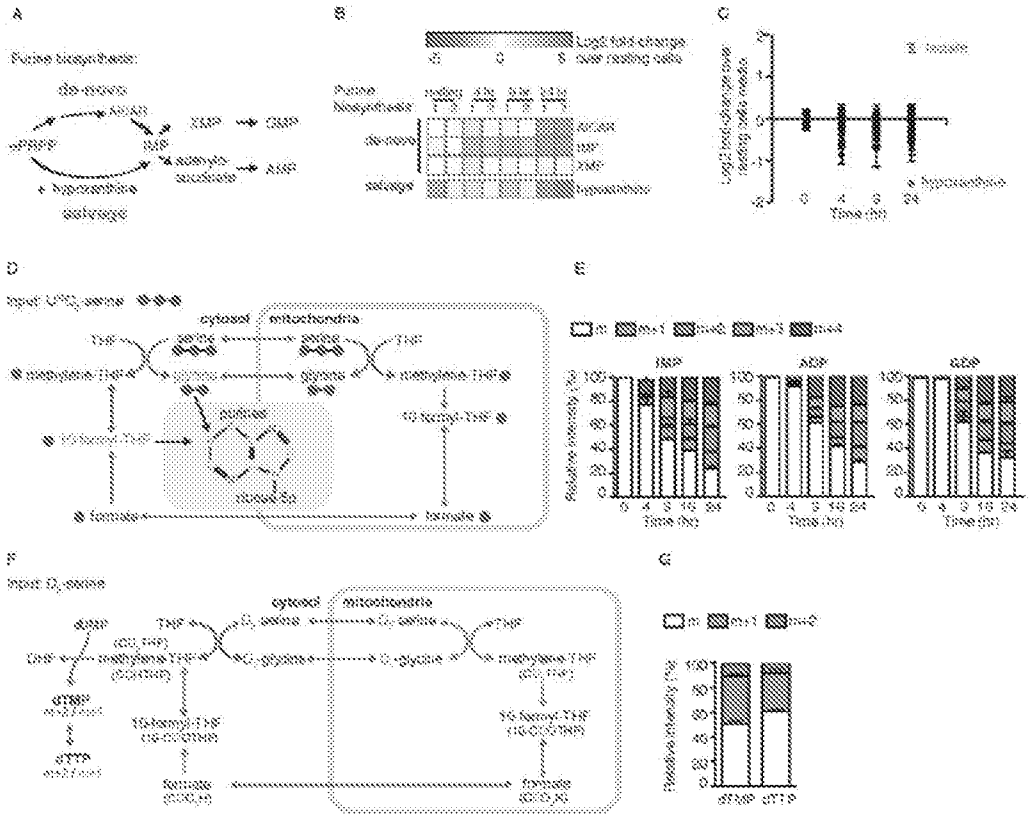

A
protein level z-score > 1SD above mean distribution
protein level z-score within mean distribution
protein level z-score >1SD below mean distribution
Arginine
Argininosuccinate
fatty acids
glutamine
ornithine
citrulline
urea cycle
glutamine
β-oxidation
CPT1A
acetyl-CoA
dihydroorotate
dihydroorotate
pyrimidine biosynthesis
orotate
malate
TCA cycle
SHMT2
MTHFD2
MTHFD2L
1-carbon metabolism
THF
glycine
serine
THF
SHMT1
MTHFD1
formate
formate
UMP/ CTP
aspartate
malate
acetyl-CoA
lipogenesis
ACC
pyruvate
pyruvate
B
0 hr
24 hr
DHODH
UMPS
CPT1a
ACC
PGRMC
ACTB
OTC
ASL
MDH2
OGDH
PGRMC
ACTB
SHMT2
MTHFD2
SHMT1
MTHFD2L
PGRMC
ACTB
C
Naive Mog specific CD4+ T cell transfer (i.v.)
MOG/CFA (s.c.)
Time (days)
analysis of CD4+ T cell population in the draining lymph nodes
D
day-2
day-0
day-4
0.6%
2.4%
14.9%
TCR Vα3.2
TCR Vβ11
E
recipient T cells
mog-specific T cells
% MOG+ cells
day-2
day-0
day-4
F
recipient T cells
mog-specific T cells
day-2
day-0
day-4
CD69
G
recipient T cells
mog-specific T cells
1-carbon metabolism
Pyrimidine biosynthesis
cell size
Shmt1
Mthfd1
Shmt2
Mthfd2
Mtrfr
Dhodh
Cad
Umps
day-2
day-0
day-4
FSC

Figure 8


A
B
C
D
E
F
G
cytosol
mitochondria
serine
glycine
formate
Time (h)

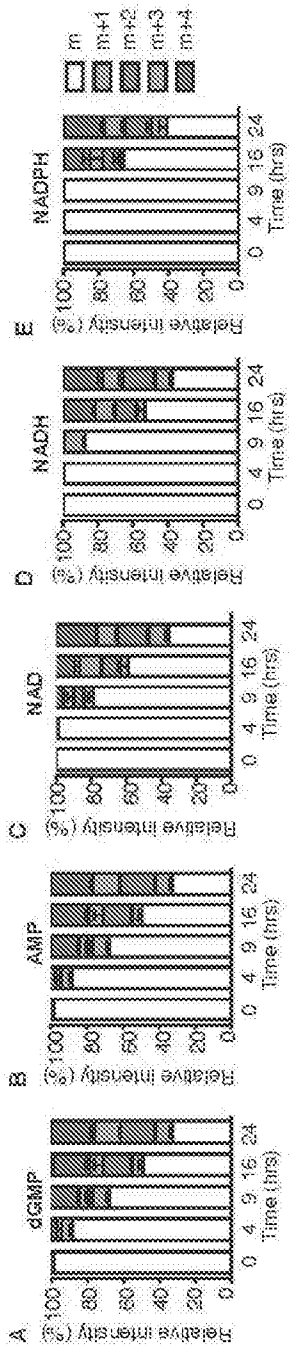

A
dGMP
B
AMP
C
NAD
D
NADH
E
NADPH
Relative Intensity (%)
Time (hrs)
0
4
9
16
24
100
80
60
40
20
m
m+1
m+2
m+3
m+4

Figure 9

Figure 10

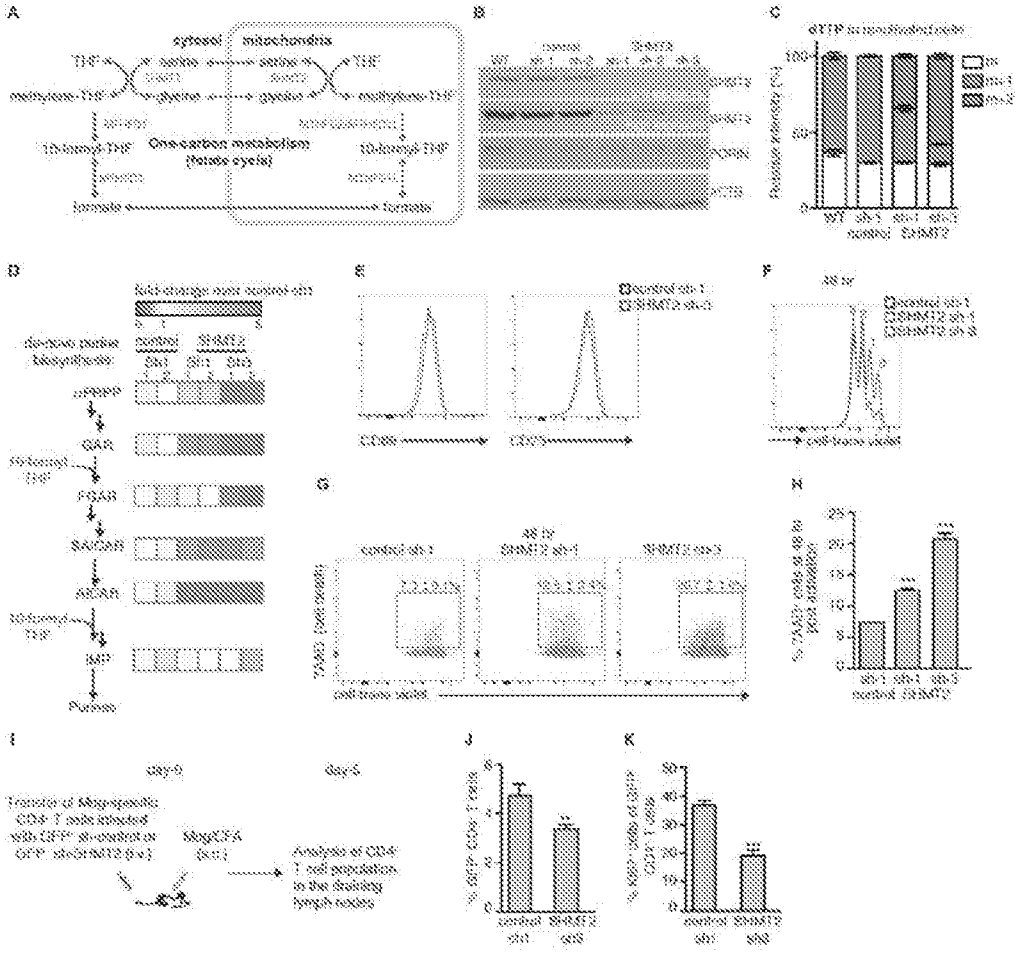


Figure 11

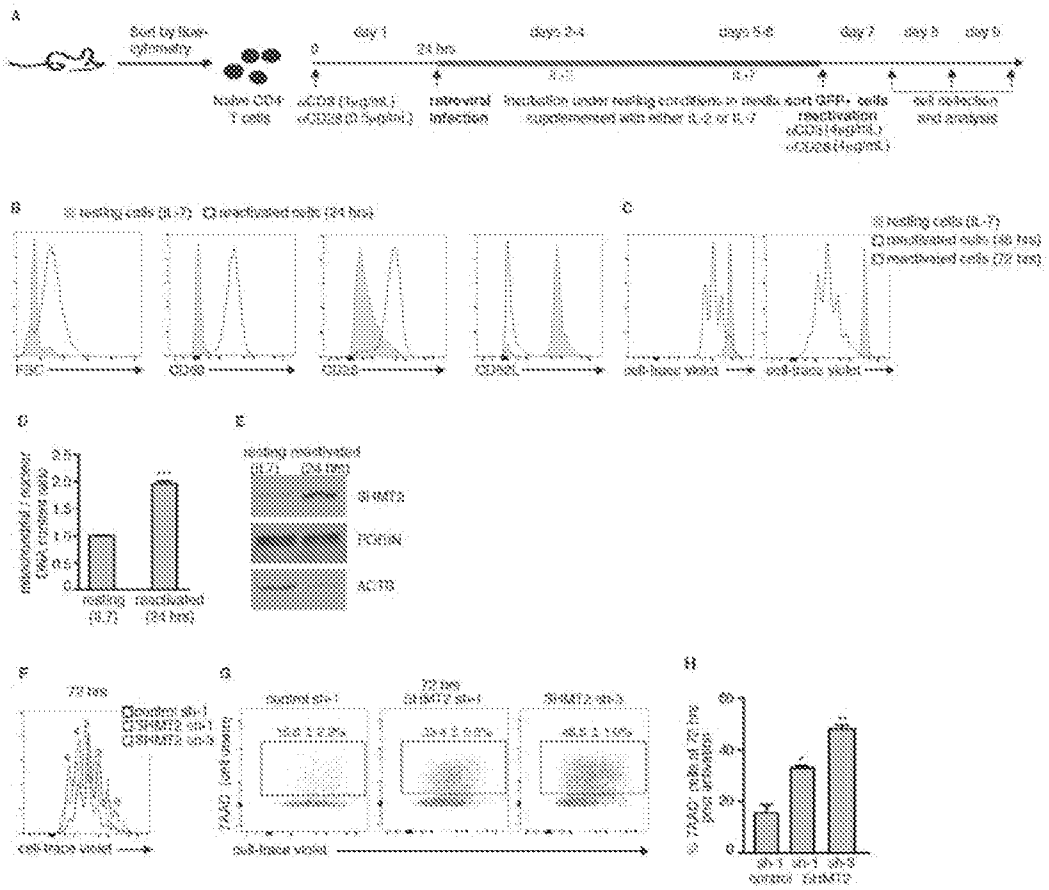


Figure 12

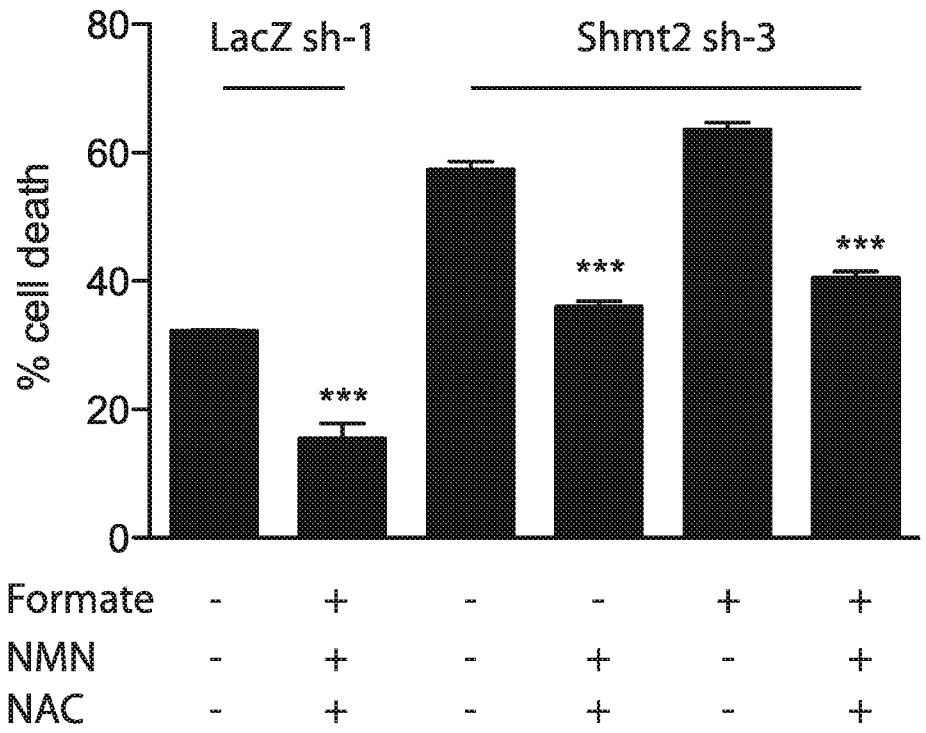


Figure 13

SHMT1

serine hydroxymethyltransferase 1 (soluble) [Homo sapiens]

NCBI Reference Sequence: NP_004160.3

```
1   mtmpvngahk dadlwsshdk mlaqplkdsd vevyniikke snrqrvglel iasenfasra
61  vlealgscln nkysegypgq ryyggtefid eletlcqkra lqaykldpqc wgvnvqpysg
121 spanfavyta lvephgrimg ldlpdgghlt hgfmtdkkki satsiffesm pykvnpdtgy
181 inydqleena rlfhpkliia gtscysrnle yarlrkiade ngaylmadma hisglvaagv
241 vpspfehchv vttttnktlr gcragmifyr kgvksvdpkt gkeilynles linsavfpgl
301 qggphnhaia gvavalkqam tlefkvyqhq vvancralse altelgykiv tggsdnhlil
361 vdlrskgtdg graekvleac siacnkntcp gdrsalrpsg lrlgtpalts rgllekdfqk
421 vahfihrgie ltlqiqsdtg vratlkefke rlagdkyqaa vqalreeves faslfplpgl
481 pdf
```

Figure 14

SHMT2

serine hydroxymethyltransferase 2 (mitochondrial) [Homo sapiens]

NCBI Reference Sequence: NP_683718.1

```
1   mtmpvngahk dadlwsshdk mlaqplkdsd vevyniikke snrqrvglel iasenfasra
61  vlealgscln nkysegypgq ryyggtefid eletlcqkra lqaykldpqc wgvnvqpysg
121 spanfavyta lvephgrimg ldlpdgghlt hgfmtdkkki satsiffesm pykvnpdtgy
181 inydqleena rlfhpkliia gtscysrnle yarlrkiade ngaylmadma hisglvaagv
241 vpspfehchv vtttthktlr gcragmifyr kgvavalkqa mtlefkvyqh qvvancrals
301 ealtelgyki vtggsdnhli lvdlrskgtd ggraekvlea csiacnkntc pgdrsalrps
361 glrlgtpalt srgllekdfq kvahfihrgi eltlqiqsdt gvratlkefk erlagdkyqa
421 avqalreeve sfaslfplpg lpdf
```

Figure 15

MTHFD1

methylenetetrahydrofolate dehydrogenase (NADP+ dependent) 1, methenyltetrahydrofolate cyclohydrolase, formyltetrahydrofolate synthetase [Homo sapiens]

NCBI Reference Sequence: NP_005947.3

```
1   mapaeilngk eisaqirarl knqvtqlkeq vpgftprlai lqvgnrddsn lyinvklkaa
61  eeigikathi klprtttese vmkyitslne dstvhgflvq lpldsensin teevinaiap
121 ekdvdgltsi nagklargdl ndcfipctpk gcleliketg vpiagrhavv vgrskivgap
181 mhdlllwnna tvttchskta hldeevnkgd ilvvatgqpe mvkgewikpg aividcginy
241 vpddkkpngr kvvgdvayde akerasfitp vpggvgpmtv amlmqstves akrflekfkp
301 gkwmiqynnl nlktpvpsdi disrsckpkp igklareigl lseevelyge tkakvllsal
361 erlkhrpdgk yvvvtgitpt plgegksttt iglvqalgah lyqnvfacvr qpsqgptfgi
421 kggaagggys qvipmeefnl hltgdihait aannlvaaai darifheltq tdkalfnrlv
481 psvngvrrfs diqirrlkrl giektdpttl tdeeinrfar ldidpetitw qrvldtndrf
541 lrkitigqap tekghtrtaq fdisvaseim avlalttsle dmrerlgkmv vasskkgepv
601 saedlgvsga ltvlmkdaik pnlmqtlegt pvfvhagpfa niahgnssii adrialklvg
661 pegfvvteag fgadigmekf fnikcrysgl cphvvvlvat vralkmhggg ptvtaglplp
721 kayiqenlel vekgfsnlkk qienarmfgi pvvvavnafk tdteseldli srlsrehgaf
781 davkcthwae ggkgalalaq avqraaqaps sfqllydlkl pvedkiriia qkiygaddie
841 llpeaqhkae vytkqgfgnl picmakthls lshnpeqkgv ptgfilpird irasvgagfl
901 yplvgtmstm pglptrpcfy didldpeteq vnglf
```

Figure 16

MTHFD2

methylenetetrahydrofolate dehydrogenase (NADP+ dependent) 2, methenyltetrahydrofolate cyclohydrolase [Homo sapiens]

NCBI Reference Sequence: NP_006627.2

```
1   maatslmsal aarllqpahs cslrlrpfhl aavrneavvi sgrklaqqik qevrqeveew
61  vasgnkrphl svilvgenpa shsyvlnktr aaavvginse timkpasise eellnliinkl
121 nnddnvdgll vqlplpehid erricnavsp dkdvdgfhvi nvgrmcldqy smlpatpwgv
181 weiikrtgip tlgknvvvag rsknvgmpia mllhtdgahe rpggdatvti shrytpkeql
241 kkhtiladiv isaagipnli tadmikegaa vidvginrvh dpvtakpklv gdvdfegvrq
301 kagyitpvpg gvgpmtvaml mkntiiaakk vlrleerevl kskelgvatn
```

Figure 17

MTHFD1L

methylenetetrahydrofolate dehydrogenase (NADP+ dependent) 1-like [Homo sapiens]

NCBI Reference Sequence: NP_001229696.1

```
1   mgtrlplvlr qlrrppqppg pprrlrvpcr assggggggg ggregllgqr rpqdgqarss
61  cspggrtpaa rdsivreviq nskevlsllq eknpafkpvl aiiqagddnl mqeinqnlae
121 eaglnithic lppdsseaei ideilkined trvhglalqi senlfsnkvl nalkpekdvd
181 gvtdinlgkl vrgdahecfv spvakaviel leksvgvnld gkkilvvgah gsleaalqcl
241 fqrkgsmtms iqwktrqlqs klheadivvl gspkpeeipl twiqpgttvl ncshdflsgk
301 vgcgsprihf gglieeddvi llaaalriqn mvssgrrwlr eqqhrrwrlh clklqplspv
361 psdieisrgq tpkavdvlak eiglladeie iygkskakvr lsvlerlkdq adgkyvlvag
421 itptplgegk stvtiglvqa ltahlnvnsf aclrqpsqgp tfgvkggaag ggyaqvipme
481 efnlhltgdi haitaannll aaaidtrilh entqtdkaly nrlvplvngv refseiqlar
541 lkklginktd pstlteeevs kfarldidps titwqrvldt ndrflrkiti gqgntekghy
601 rqaqfdiava seimavlalt dsladmkarl grmvvasdks gqpvtaddlg vtgaltvlmk
661 daikpnlmqt legtpvfvha gpfaniahgn ssvladkial klvgeegfvv teagfgadig
721 mekffnikcr asglvpnvvv lvatvralkm hgggpsvtag vplkkeytee niqlvadgcc
781 nlqkqiqitq lfgvpvvval nvfktdtrae idlvcelakr agafdavpcy hwsvggkgsv
841 dlaravreaa skrsrfqfly dvqvpivdki rtiaqavyga kdielspeaq akidrytqqg
901 fgnlpicmak thlslshqpd kkgvprdfil pisdvrasig agfiyplvgt mstmpglptr
961 pcfydidldt eteqvkglf
```

Figure 18

MTHFD2L

methylenetetrahydrofolate dehydrogenase (NADP+ dependent) 2-like [Homo sapiens]

NCBI Reference Sequence: NP_001138450.1

```
1   mtvpvrgfsl lrgrlgrapa lgrstapsvr apgepgsafr gfrssgvrhe aiiisgtema
61  khiqkeiqrg veswvslgnr rphlsiilvg dnpashtyvr nkiraasavg icselilkpk
121 dvsqeelldv tdqlnmdprv sgilvqlplp dhvderticn giapekdvdg fhiinigrlc
181 ldqhslipat asavweiikr tgiqtfgknv vvagrsknvg mpiamllhtd geherpggda
241 tvtiahrytp keqlkihtql adiiivaagi pklitsdmvk egaavidvgi nyvhdpvtgk
301 tklvgdvdfe avkkkagfit pvpggvgpmt vamllkntll aakkiiy
```

Figure 19

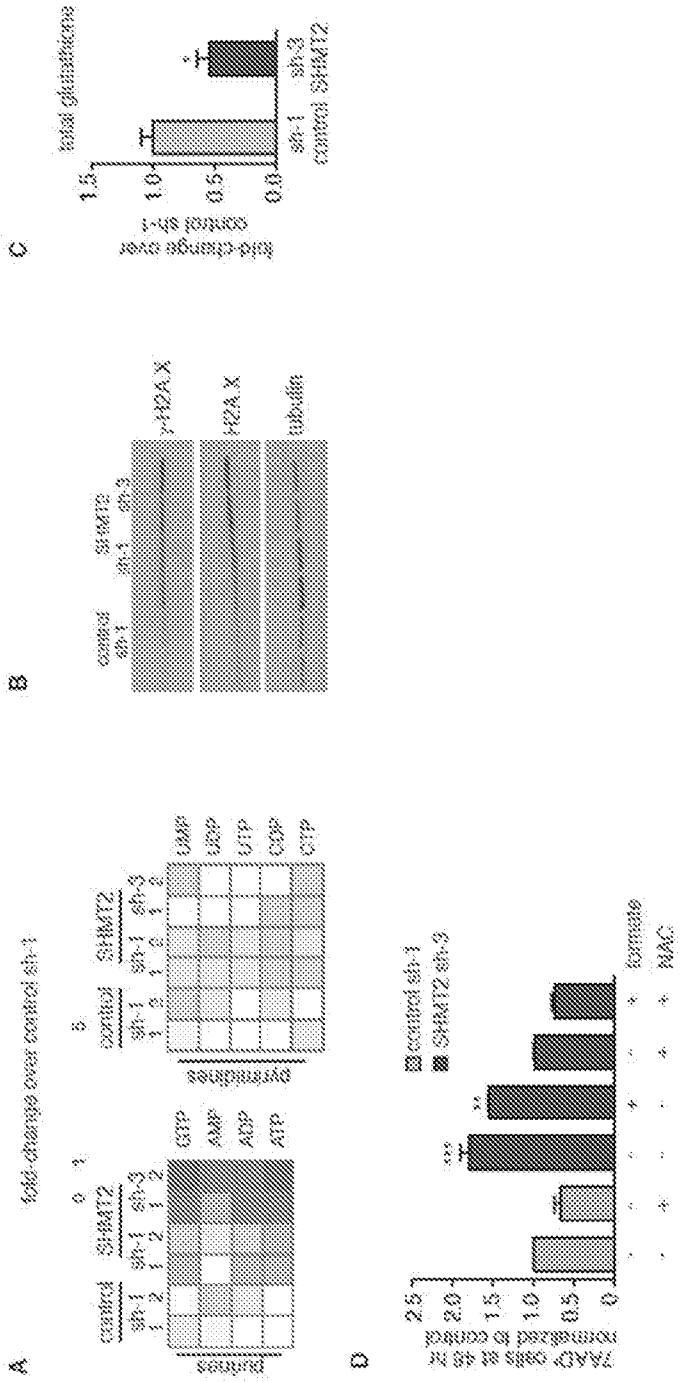

A
fold-change over control sh-1
control
SHMT2
sh-1
sh-3
purines
pyrimidines
GTP
AMP
ADP
ATP
UMP
UDP
UTP
CDP
CTP
B
control sh-1
SHMT2 sh-1
SHMT2 sh-3
γ-H2A.X
H2A.X
tubulin
C
fold-change over control sh-1
total glutathione
control
SHMT2
sh-1
sh-3
D
control sh-1
SHMT2 sh-3
formate
NAC

Figure 20

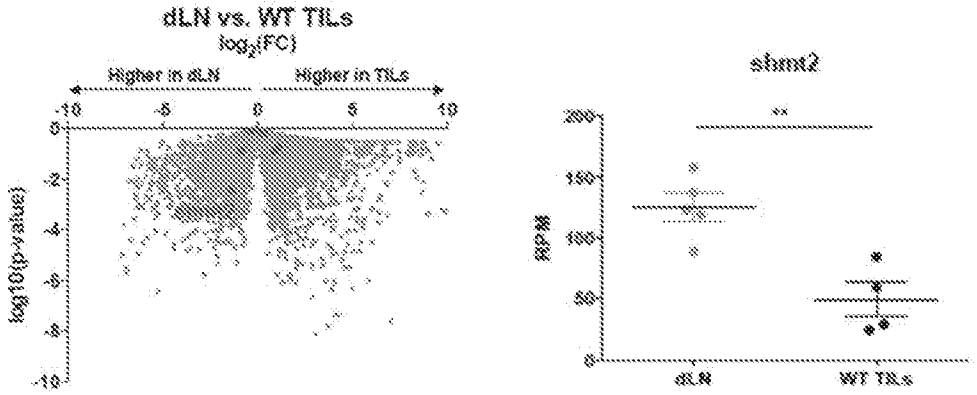


Figure 21

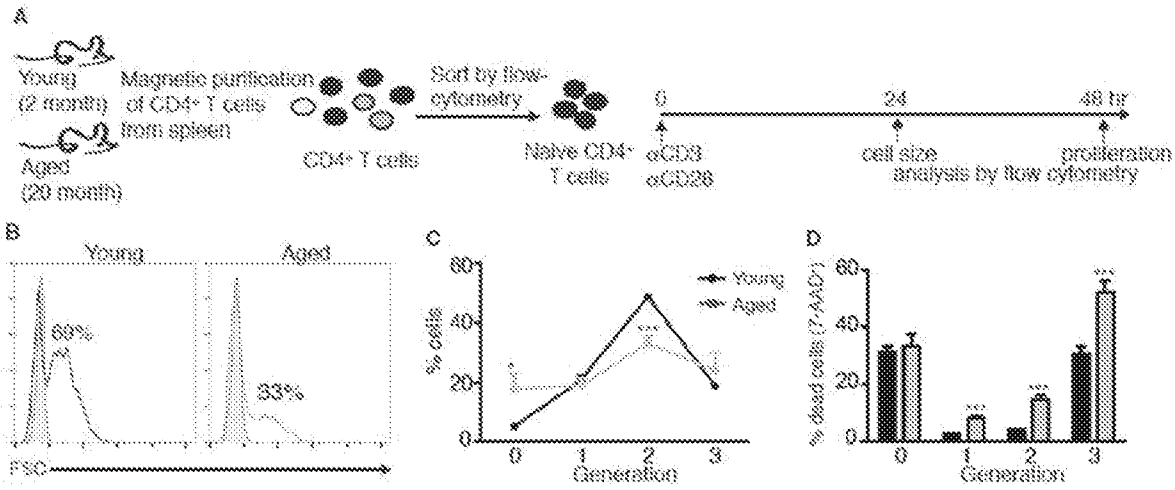


Figure 22

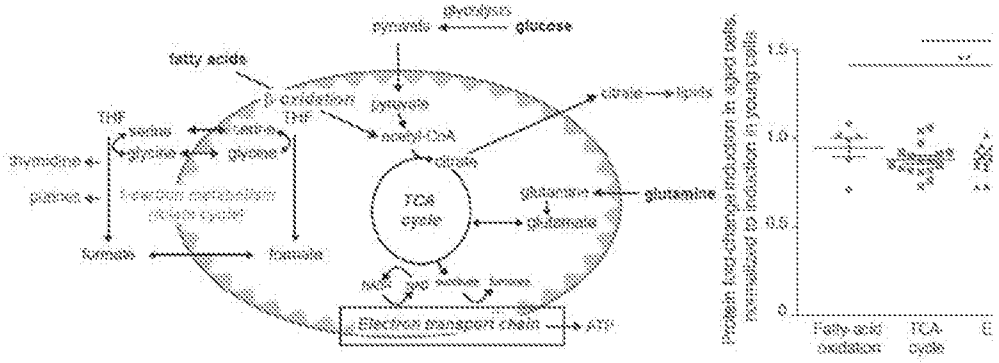
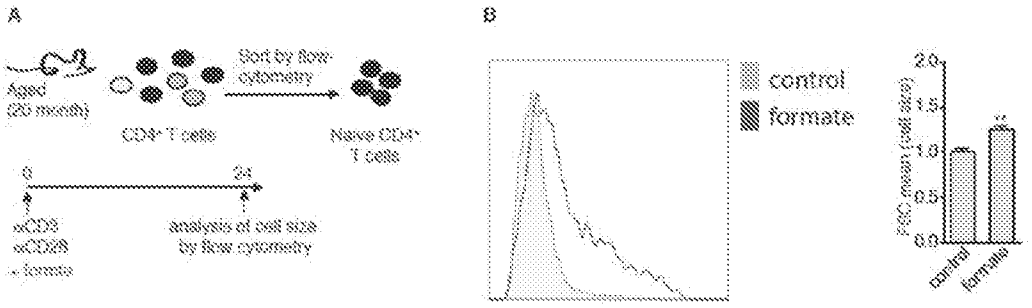


Figure 23


A
Aged
(20 month)
Sort by flow cytometry
CD4+ T cells
Naive CD4+
T cells
0
2d
αCD3
αCD28
+ formate
analysis of cell size
by flow cytometry
B
control
formate
2.0
1.5
1.0
0.5
0.0
control
formate

INTERNATIONAL SEARCH REPORT

International application No
PCT/US2017/021727

A. CLASSIFICATION OF SUBJECT MATTER
INV. C12N15/113 A61P37/02 C12Q1/68 G01N33/573
ADD.

According to International Patent Classification (IPC) or to both national classification and IPC

B. FIELDS SEARCHED

Minimum documentation searched (classification system followed by classification symbols)
C12N

Documentation searched other than minimum documentation to the extent that such documents are included in the fields searched

Electronic data base consulted during the international search (name of data base and, where practicable, search terms used)
EPO-Internal, WPI Data, EMBASE, BIOSIS

C. DOCUMENTS CONSIDERED TO BE RELEVANT

Category*	Citation of document, with indication, where appropriate, of the relevant passages	Relevant to claim No.
X	ANTONIOS TRAKATELLIS ET AL: "Pyridoxine deficiency: new approaches in immunosuppression and chemotherapy", POSTGRAD MED J, vol. 73, 1 January 1997 (1997-01-01), pages 617-622, XP055374298, the whole document -----	1-18
X	WO 2005/012577 A1 (IRM LLC [US]; SHAH KAVITA [US]; KIM SUNGJOON [US]) 10 February 2005 (2005-02-10) page 1, paragraph 2 page 24, line 3 - line 6; example 4 page 25, line 24 - line 28 ----- -/--	1-18

[X] Further documents are listed in the continuation of Box C.

[X] See patent family annex.

* Special categories of cited documents :

"A" document defining the general state of the art which is not considered to be of particular relevance

"E" earlier application or patent but published on or after the international filing date

"L" document which may throw doubts on priority claim(s) or which is cited to establish the publication date of another citation or other special reason (as specified)

"O" document referring to an oral disclosure, use, exhibition or other means

"P" document published prior to the international filing date but later than the priority date claimed

"T" later document published after the international filing date or priority date and not in conflict with the application but cited to understand the principle or theory underlying the invention

"X" document of particular relevance; the claimed invention cannot be considered novel or cannot be considered to involve an inventive step when the document is taken alone

"Y" document of particular relevance; the claimed invention cannot be considered to involve an inventive step when the document is combined with one or more other such documents, such combination being obvious to a person skilled in the art

"&" document member of the same patent family

Date of the actual completion of the international search	Date of mailing of the international search report
19 May 2017	03/08/2017

Name and mailing address of the ISA/	Authorized officer
European Patent Office, P.B. 5818 Patentlaan 2 NL - 2280 HV Rijswijk Tel. (+31-70) 340-2040, Fax: (+31-70) 340-3016	Wiame, Ilse

1

Form PCT/ISA/210 (second sheet) (April 2005)

C(Continuation). DOCUMENTS CONSIDERED TO BE RELEVANT

Category*	Citation of document, with indication, where appropriate, of the relevant passages	Relevant to claim No.
X	BRIAN ASTRY ET AL: "Celastrol, a Chinese herbal compound, controls autoimmune inflammation by altering the balance of pathogenic and regulatory T cells in the target organ", CLINICAL IMMUNOLOGY, vol. 157, no. 2, 1 April 2015 (2015-04-01) , pages 228-238, XP055332621, US ISSN: 1521-6616, DOI: 10.1016/j.clim.2015.01.011 abstract page 229, column 1, paragraph 3 page 237, column 1, line 4 - line 7 -----	1-4, 8-11,16, 17
X	RADHAMANI KANNAIYAN ET AL: "Molecular targets of celastrol derived from Thunder of God Vine: Potential role in the treatment of inflammatory disorders and cancer", CANCER LETTERS, NEW YORK, NY, US, vol. 303, no. 1, 28 October 2010 (2010-10-28), pages 9-20, XP028152697, ISSN: 0304-3835, DOI: 10.1016/J.CANLET.2010.10.025 [retrieved on 2010-11-01] abstract; table 1 page 11 - page 12 -----	1-4, 8-13, 16-18
A	WO 2014/150688 A1 (GEN HOSPITAL CORP [US]) 25 September 2014 (2014-09-25) cited in the application example 13 page 58, line 11 - line 12 -----	1-18
A	MICHAEL D. BUCK ET AL: "T cell metabolism drives immunity", THE JOURNAL OF EXPERIMENTAL MEDICINE, vol. 212, no. 9, 10 August 2015 (2015-08-10), pages 1345-1360, XP055374549, US ISSN: 0022-1007, DOI: 10.1084/jem.20151159 page 1353, column 2, paragraph 2 ----- -/--	1-18

1

C(Continuation). DOCUMENTS CONSIDERED TO BE RELEVANT

Category*	Citation of document, with indication, where appropriate, of the relevant passages	Relevant to claim No.
X,P	RON-HAREL NOGA ET AL: "Mitochondrial Biogenesis and Proteome Remodeling Promote One-Carbon Metabolism for T Cell Activation", CELL METABOLISM, CELL PRESS, UNITED STATES, vol. 24, no. 1, 12 July 2016 (2016-07-12), pages 104-117, XP029638760, ISSN: 1550-4131, DOI: 10.1016/J.CMET.2016.06.007 the whole document	1-18
X,P	WO 2016/145252 A1 (UNIV PRINCETON [US]) 15 September 2016 (2016-09-15) the whole document	1-18
A	M. D. KELLER ET AL: "Severe Combined Immunodeficiency Resulting From Mutations in MTHFD1", PEDIATRICS, vol. 131, no. 2, 6 January 2013 (2013-01-06), pages e629-e634, XP055374563, ISSN: 0031-4005, DOI: 10.1542/peds.2012-0899 abstract	1

1

INTERNATIONAL SEARCH REPORT

International application No.
PCT/US2017/021727

Box No. I Nucleotide and/or amino acid sequence(s) (Continuation of item 1.c of the first sheet)

1. With regard to any nucleotide and/or amino acid sequence disclosed in the international application, the international search was carried out on the basis of a sequence listing:

   a. ☐ forming part of the international application as filed:

      ☐ in the form of an Annex C/ST.25 text file.

      ☐ on paper or in the form of an image file.

   b. ☐ furnished together with the international application under PCT Rule 13*ter*.1(a) for the purposes of international search only in the form of an Annex C/ST.25 text file.

   c. ☒ furnished subsequent to the international filing date for the purposes of international search only:

      ☒ in the form of an Annex C/ST.25 text file (Rule 13*ter*.1(a)).

      ☐ on paper or in the form of an image file (Rule 13*ter*.1(b) and Administrative Instructions, Section 713).

2. ☐ In addition, in the case that more than one version or copy of a sequence listing has been filed or furnished, the required statements that the information in the subsequent or additional copies is identical to that forming part of the application as filed or does not go beyond the application as filed, as appropriate, were furnished.

3. Additional comments:

INTERNATIONAL SEARCH REPORT

International application No.
PCT/US2017/021727

Box No. II Observations where certain claims were found unsearchable (Continuation of item 2 of first sheet)

This international search report has not been established in respect of certain claims under Article 17(2)(a) for the following reasons:

1. ☐ Claims Nos.:
because they relate to subject matter not required to be searched by this Authority, namely:

2. ☐ Claims Nos.:
because they relate to parts of the international application that do not comply with the prescribed requirements to such an extent that no meaningful international search can be carried out, specifically:

3. ☐ Claims Nos.:
because they are dependent claims and are not drafted in accordance with the second and third sentences of Rule 6.4(a).

Box No. III Observations where unity of invention is lacking (Continuation of item 3 of first sheet)

This International Searching Authority found multiple inventions in this international application, as follows:

see additional sheet

1. ☐ As all required additional search fees were timely paid by the applicant, this international search report covers all searchable claims.

2. ☐ As all searchable claims could be searched without effort justifying an additional fees, this Authority did not invite payment of additional fees.

3. ☐ As only some of the required additional search fees were timely paid by the applicant, this international search report covers only those claims for which fees were paid, specifically claims Nos.:

4. ☒ No required additional search fees were timely paid by the applicant. Consequently, this international search report is restricted to the invention first mentioned in the claims; it is covered by claims Nos.:

1-18

Remark on Protest

☐ The additional search fees were accompanied by the applicant's protest and, where applicable, the payment of a protest fee.

☐ The additional search fees were accompanied by the applicant's protest but the applicable protest fee was not paid within the time limit specified in the invitation.

☐ No protest accompanied the payment of additional search fees.

FURTHER INFORMATION CONTINUED FROM PCT/ISA/ 210

This International Searching Authority found multiple (groups of) inventions in this international application, as follows:

1. claims: 1-18

A method of treating or preventing an autoimmune disease, an inflammatory disease, a graft-versus host disease or organ transplant rejection in a subject comprising administering to the subject an agent that inhibits the one-carbon metabolic pathway.

---

2. claims: 19-32

A method of treating or preventing a disease or disorder associated with impairment of the one-carbon metabolic pathway in a subject comprising administering to the subject an agent that increases the activity or expression of SHMT1, SHMT2, MTHFD1, MTHFD2, MTHFD1L or MTHFD2L in the subject.

---

3. claims: 33-40, 76-87

A method of detecting T cell activation comprising detecting the level of SHMT1, SHMT2, MTHFD1, MTHFD2, MTHFD1L or MTHFD2L in a T cell.
A method of detecting T cell exhaustion in a subject comprising detecting the level of SHMT1, SHMT2, MTHFD1, MTHFD2, MTHFD1L or MTHFD2L expressed by T cells in the subject.

---

4. claims: 41-56

A method of detecting an autoimmune disease, an inflammatory disease, a graft-versus host disease or organ transplant rejection in a subject comprising detecting the level of SHMT1, SHMT2, MTHFD1, MTHFD2, MTHFDIL or MTHFD2L expressed by T cells in the subject.

---

5. claims: 57-75

A method of determining the efficacy of an immunotherapy in a subject comprising detecting the level of SHMT1, SHMT2, MTHFD1, MTHFD2, MTHFD1L or MTHFD2L expressed by T cells in the subject.

---

6. claims: 88-115

A method of treating or preventing a cancer in a subject comprising administering to the subject an agent that increases the activity or expression of SHMT2 in the subject.

A method of increasing tumor infiltrating T cell activity or function in a subject comprising administering to the subject an agent that increases the activity or expression of SHMT2 in the subject.
A method of treating a tumor in a subject comprising administering to the subject an agent that increases the activity or expression of SHMT2 in the subject.

---

7. claims: 116-119

A method of reducing age-related T cell dysfunction in a subject comprising administering to the subject an agent that activates one-carbon metabolic pathway.
A method of increasing T cell growth comprising administering to the subject an agent that increases the activity or expression of SHMT2 in the subject.

INTERNATIONAL SEARCH REPORT

Information on patent family members

International application No
PCT/US2017/021727

Patent document cited in search report	Publication date	Patent family member(s)	Publication date
WO 2005012577 A1	10-02-2005	US 2005118663 A1	02-06-2005
		WO 2005012577 A1	10-02-2005
WO 2014150688 A1	25-09-2014	AU 2014235761 A1	24-09-2015
		CA 2904350 A1	25-09-2014
		EP 2971153 A1	20-01-2016
		JP 2016514136 A	19-05-2016
		SG 11201507366R A	29-10-2015
		US 2016032401 A1	04-02-2016
		WO 2014150688 A1	25-09-2014
WO 2016145252 A1	15-09-2016	NONE	